

Rowan University

Rowan Digital Works

---

Theses and Dissertations


---

6-5-2017

## Data analysis and processing techniques for remaining useful life estimations

John Scott Bucknam  
*Rowan University*

Follow this and additional works at: <https://rdw.rowan.edu/etd>

 Part of the [Computer Sciences Commons](#), and the [Operations Research, Systems Engineering and Industrial Engineering Commons](#)

---

### Recommended Citation

Bucknam, John Scott, "Data analysis and processing techniques for remaining useful life estimations" (2017). *Theses and Dissertations*. 2430.  
<https://rdw.rowan.edu/etd/2430>

This Thesis is brought to you for free and open access by Rowan Digital Works. It has been accepted for inclusion in Theses and Dissertations by an authorized administrator of Rowan Digital Works. For more information, please contact [graduateresearch@rowan.edu](mailto:graduateresearch@rowan.edu).

**DATA ANALYSIS AND PROCESSING TECHNIQUES FOR REMAINING  
USEFUL LIFE ESTIMATIONS**

by  
John S. Bucknam Jr.

A Thesis

Submitted to the  
Department of Computer Science  
College of Science and Mathematics  
in partial fulfillment of the requirement  
for the degree of  
Master of Science in Computer Science  
at  
Rowan University  
May 26, 2017

Thesis Chair: Ganesh Baliga, PhD.

© 2017 John S. Bucknam Jr.

## Acknowledgments

I would like to thank Dr. Ganesh Baliga for keeping on track as I finished this paper, as well as Nick LaPosta for those 2:00 AM moments. I would also like to thank my family for supporting me throughout my Bachelors and Masters.

## Abstract

John S. Bucknam Jr.

DATA ANALYSIS AND PROCESSING TECHNIQUES FOR REMAINING USEFUL  
LIFE ESTIMATIONS

2016-2017

Ganesh Baliga, PhD.

Master of Science in Computer Science

In the field of engineering, it is important to understand different engineering systems and components, not only in how they currently performs, but also how their performance degrades over time. This extends to the field of prognostics, which attempts to predict the future of a system or component based on its past and present states. A common problem in this field is the estimation of remaining useful life, or how long a system or component functionality will last. The well-known datasets for this problem are the PHM and C-MAPSS datasets. These datasets contain simulated sensor data for different turbofan engines generated over time, and have been used to study estimations of remaining useful life.

In thesis, we study estimations of remaining useful life using different methods of data analytics, preprocessing, post-processing, different target functions used for training models, and their combinations. We compared their performance primarily using scores from the 2008 Prognostics and Health Management Competition. Our basic feedforward neural network with aggregation outperforms previously competitors and other modern methods. Our results also gave us a ranking between the top 10 and 15 based on a 2014 benchmark using the PHM dataset. We have improved the results of previously, published methods, primarily focusing on the Prognostics Health Management competition score of our results for better comparisons.

## Table of Contents

Abstract . . . . .	iv
List of Figures . . . . .	viii
List of Tables . . . . .	xi
Chapter 1: Introduction . . . . .	1
1.1 Background . . . . .	1
1.2 Problem Description . . . . .	2
1.3 Motivation . . . . .	4
1.4 Current Methods . . . . .	5
Chapter 2: Understanding the Data and Experiments . . . . .	8
2.1 General Information . . . . .	8
2.2 RUL Target Function . . . . .	11
2.3 Fault Mode . . . . .	13
2.4 Operating Conditions . . . . .	15
2.5 Testing Data . . . . .	18
2.6 Experiment Layout . . . . .	19
2.6.1 Model layout. . . . .	20
Chapter 3: Data and Target Function Processing . . . . .	22
3.1 Overview . . . . .	22
3.2 Basic Normalization . . . . .	24
3.3 Regime Partitioning . . . . .	26
3.3.1 Clustering. . . . .	29
3.3.2 Purpose. . . . .	30
3.3.3 Issues. . . . .	31
3.4 Data Selection . . . . .	31
3.5 Filtering and Aggregation . . . . .	32

## Table of Contents (Continued)

3.5.1	Regression. . . . .	33
3.5.2	Kalman filters. . . . .	34
3.5.3	Butterworth filter. . . . .	34
3.5.4	Savitzky-Golay filter. . . . .	34
3.6	Target Function Transformations . . . . .	35
3.6.1	Kinked function. . . . .	36
3.6.2	Scaled target function. . . . .	36
Chapter 4:	Experiments . . . . .	38
4.1	Baseline Models . . . . .	38
4.1.1	Results. . . . .	39
4.2	Max-Multiplier Experiment . . . . .	40
4.2.1	Hypothesis. . . . .	40
4.2.2	Methodology. . . . .	40
4.2.3	Results. . . . .	41
4.3	Cycle Number Inclusion Experiment . . . . .	42
4.3.1	Hypothesis. . . . .	42
4.3.2	Methodology. . . . .	42
4.3.3	Results. . . . .	43
4.4	Classifiers Exploration . . . . .	43
4.4.1	Hypothesis. . . . .	45
4.4.2	Methodology. . . . .	45
4.4.3	Results. . . . .	46
4.5	Regime Partitioning . . . . .	47
4.5.1	Hypothesis. . . . .	48
4.5.2	Methodology. . . . .	48

## Table of Contents (Continued)

4.5.3	Results. . . . .	49
4.6	Aggregation via Filtering . . . . .	54
4.6.1	Hypothesis. . . . .	54
4.6.2	Methodology. . . . .	54
4.6.3	Results. . . . .	55
Chapter 5:	Conclusion . . . . .	62
5.1	Future Work . . . . .	63
5.1.1	Transferability of datasets. . . . .	63
5.1.2	Searching for a better scaling multiplier. . . . .	63
5.1.3	Incrementing our target function. . . . .	64
5.1.4	Preprocessed aggregation. . . . .	65
References	. . . . .	66



## List of Figures

Figure	Page
Figure 1. Scoring Equation . . . . .	3
Figure 2. C-MAPSS 1 - Unit 1 Sensors Example (Expanded Normalization from chapter 3) . . . . .	11
Figure 5. RUL Equation . . . . .	12
Figure 3. Cycle Number of Data Points in PHM TRAIN Unit 1 . . . . .	12
Figure 4. RUL Target of Data Points in PHM TRAIN Unit 1 . . . . .	12
Figure 6. C-MAPSS 3 - Unit 54 (Expanded Normalization from chapter 3) . . . . .	14
Figure 7. C-MAPSS 4 - Unit 70 (Regime Partitioning from chapter 3) . . . . .	15
Figure 8. PHM Unit 1 - Expanded Normalization from chapter 3 . . . . .	16
Figure 9. PCA Components of C-MAPSS 1 Train . . . . .	17
Figure 10. PCA Components of PHM Train . . . . .	17
Figure 11. RUL Target of Data Points in PHM TRAIN Unit 1 . . . . .	17
Figure 12. Standardization . . . . .	24
Figure 13. Feature Scaling . . . . .	25
Figure 14. Expanded Standardization . . . . .	25
Figure 15. Expanded Feature Scaling . . . . .	25
Figure 16. Normalization Comparison (a) Original (b) Standardization (c) Feature Scaling . . . . .	26
Figure 17. Expanded Normal C-MAPSS 1 . . . . .	26
Figure 18. Expanded Scaled C-MAPSS 1 [-1, 1] . . . . .	26
Figure 19. Original PHM Train . . . . .	27
Figure 20. PHM Train Operating Conditions . . . . .	28
Figure 21. Regime-Partitioned Standardization . . . . .	28

Figure 22.	Regime-Partitioned Feature Scaling . . . . .	28
Figure 23.	Regime-Partitioned Normal PHM Train . . . . .	29
Figure 24.	Regime-Partitioned Scaled PHM Train . . . . .	29
Figure 25.	PHM Train - Unit 1 Sensors (a) Upwards {2,3,4,8,11,13,15,18} (b) Downwards {7,12,20,21} (c) Shifting {9,14} . . . . .	31
Figure 26.	C-MAPSS 1 Train - Unit 1 Sensors (a) Upwards {2,3,4,8,11,13,15,18} (b) Downwards {7,12,20,21} (c) Shifting {9,14} . . . . .	32
Figure 27.	PHM Train - Unit 1 Kinked Target Function . . . . .	35
Figure 28.	Kinked Equation . . . . .	36
Figure 29.	PHM Train - Unit 1 Scaled Target Function . . . . .	37
Figure 30.	PHM Train Validation Set (24x13x13x1) . . . . .	42
Figure 31.	PHM Train Validation Set (24x13x13x1 - Dropout) . . . . .	42
Figure 32.	Accurate PHM Train Unit FNN Classifier . . . . .	44
Figure 33.	Inaccurate PHM Train Unit FNN Classifier . . . . .	44
Figure 34.	Accurate PHM Train Unit (100% Accuracy) SVC . . . . .	44
Figure 35.	Inaccurate PHM Train Unit SVC . . . . .	44
Figure 36.	PHM Test Unit FNN - No Cycle . . . . .	45
Figure 37.	PHM Test Unit FNN - Cycle . . . . .	45
Figure 38.	PHM Test Unit 31 SVM Filter . . . . .	55
Figure 39.	PHM Test Unit 31 Random Forest Filter . . . . .	55
Figure 40.	PHM Train Unit 1 Polynomial . . . . .	56
Figure 41.	PHM Test Unit 31 Polynomial . . . . .	56
Figure 42.	PHM Test Unit 150 Polynomial . . . . .	57
Figure 43.	PHM Train Unit 1 Butterworth . . . . .	57
Figure 44.	PHM Test Unit 31 Butterworth . . . . .	57

Figure 45.	PHM Test Unit 150 Butterworth . . . . .	58
Figure 46.	PHM Train Unit 1 Savitzky-Golay . . . . .	59
Figure 47.	PHM Test Unit 31 Savitzky-Golay . . . . .	59
Figure 48.	PHM Test Unit 150 Savitzky-Golay . . . . .	59

## List of Tables

Table		Page
Table 1.	Results from MLP Ensemble and Kalman Filter Approach [1] . . . . .	7
Table 2.	Description of NASA Data Repository [2] . . . . .	8
Table 3.	Minimum, Maximum, and Average Length of Series in Datasets . . . . .	13
Table 4.	Minimum and Maximum Length of Series in Test Datasets . . . . .	18
Table 5.	Baseline Models Comparisons . . . . .	39
Table 6.	Initial Neural Network Comparisons . . . . .	41
Table 7.	Cycle Number Inclusion vs. Exclusion . . . . .	43
Table 8.	SVC Classifier Comparison . . . . .	46
Table 9.	FNN Classifier Comparison . . . . .	47
Table 10.	Expanded Normalization vs Regime Partitioning . . . . .	48
Table 11.	Total RUL Score (Expanded Normalization w/ Cycle Number) . . . . .	50
Table 12.	Total RUL Score (Expanded Normalization w/o Cycle Number) . . . . .	51
Table 13.	Total RUL Score (Regime Partitioning w/ Cycle Number) . . . . .	52
Table 14.	Total RUL Score (Regime Partitioning w/o Cycle Number) . . . . .	53
Table 15.	Filter Comparison . . . . .	60

## Chapter 1

### Introduction

#### 1.1 Background

As we send more machines into the darkest depths of the ocean and the farthest reaches of space, engineers are forced to ask more questions about the functionality and performance of these systems. Although this can include such details about the past and present status of our different systems and components of a given system, wouldn't it be important for us to know how long the system will continue functioning? From these future-seeking questions we obtain the study of *prognostics*, the discipline of predicting the time of failure for a system or component.

This focus on the time of failures leads engineers to focus on the amount of time of proper functionality remaining, often referred to as the *remaining useful life (RUL)* of a component. The RUL estimation is now a standard problem for any system and is the main focus of several organizations, including the *National Aeronautics and Space Administration (NASA)* and the *Prognostics & Health Management (PHM) Society* who have promoted the field by publishing several datasets open to the public, providing the free, unrestricted access to PHM knowledge, and promoting collaboration.

In 2008, the PHM Society focused their efforts on a data challenge as a part of their PHM '08 Conference. This challenge focused on the RUL estimation of a custom dataset based on simulated turbofan engine degradation and was meant to advocate different methodologies and solutions to the problem. This research has then been expanded throughout the years, focusing on previous methodologies that are described in this paper.

## 1.2 Problem Description

The PHM data challenge consists of 3 datasets, the training dataset, the testing dataset, and the final submission dataset. The training dataset has a set of engines separated by a unit number, and has the complete run of the engine from start to failure. However, the testing and final datasets only have incomplete runs of different engines, where we know the start of the engine, but not the state of failure.

Using the training set, we are to train a model that can accurately predict the RUL for each partial engine set in our testing dataset and final dataset. This submission can be done once a day with the testing dataset, but only once with the final dataset, and is submitted through a site defined by NASA or the PHM Society.

The competitor receives a score based on the estimated RUL and actual RUL, where a larger penalty is given when the estimated RUL over-estimates the actual RUL. If the score is 0 then it is a perfect match, but due to the limited amount of information from the testing set, we find that it is common to over-estimate our data.

For instance, in the PHM testing dataset, there is an engine series with only 15 cycles given, making it more likely to be over-estimate depending on the model. Because of the exponential nature of the function, an over-estimation of 60 cycles equates to a score increase of over 400 points. Our goal is to have as low of a score as possible, but our score is an aggregate of  $d$  (defined in Figure 1) for each engine in our dataset, making the score harder to manage with larger, partial-time datasets.

For this problem, we focused on the testing dataset, as we were unable to find the

Let  $d = (EstimatedRUL - ActualRUL)$ , then

$$Score = \begin{cases} \sum_{i=1}^n e^{-\left(\frac{d_i}{a_1}\right)} - 1 & \text{for } d < 0 \\ \sum_{i=1}^n e^{\left(\frac{d_i}{a_2}\right)} - 1 & \text{for } d \geq 0 \end{cases}$$

where  $i$  is the  $i$ th engine unit of our dataset

and where  $a_1 = 13$

and  $a_2 = 10$

Figure 1. Scoring Equation

final submission site and could only submit once even if found. We also focused on 4 separate datasets generated by the *Commerical Modular Aero-Propulsion System Simulation (C-MAPSS)*, as it is related to our PHM datasets and is generated using different initial settings, giving us a different perspective of our data. Each of these separate datasets will be known by a number and the simulation used to generate them (i.e. C-MAPSS 1, C-MAPSS 2, C-MAPSS 3, C-MAPSS 4) with our PHM dataset defined simply as PHM.

Each of these datasets have a different number of fault modes and operating conditions known beforehand that affect the sensors used by our data. The operating condition further separates our sensors into separate clusters for each data point. The dataset can also increase in difficulty due to the number of fault modes, allowing more possible states of failure and a possible continuation of our data when expecting failure. More on these details are explored in chapter 2.

Each engine in our dataset is defined as a time series of data points. The engines are separated using a *unit number* that defines what engine the point belongs to in our dataset.

A *cycle number* is also used to define how many cycles (time) has passed at the given data point. There are also 3 *operating settings* that are used to define the operating condition for each data point and 21 *sensors* that primarily describe the health of our data point.

### 1.3 Motivation

Although different techniques and methods have been developed since the 2008 competition, we find that there aren't several comparisons done between them. Furthermore, not much has been done to build on top of the previous success of different methodologies. Instead, we see a large variety of algorithms used with different variations in success, and although some benchmarking has been done to expand on these different approaches [2], we would like to advance these approaches while further comparing their results.

This includes comparisons between the structure of different datasets, the performance of each dataset on various models and preprocessing methods, and the transferability of models trained among different datasets. We will compare different models on their performance and attempt to understand the effects of preprocessing has on our data. The structure of different datasets will be compared using different methods of dimensional reduction as well as comparing selected sensors commonly used.

Although several advanced models have been used with large success [3, 4], we will be focusing on simpler model for these estimations. This is to better compare basic results and to simplify our data processing and model modifications. It also allows us to better compare results from many common methods and algorithms. We also hope that this paper acts as a jumping point for future RUL estimation models and to better understand



the effects of data processing.

#### 1.4 Current Methods

After the 2008 PHM Data Challenge, three winners were announced with the best results. Each of the winners used different approaches for their solution. The first place winner used a similarity-based approach, the second place winner used a set of Recurrent Neural Networks (RNN), and the third place winner used a Multi-Layer Perceptron (MLP) ensemble with a Kalman Filter [2]. Although other methods have been described such as RULCLIPPER which uses computational geometry to compute planar polygons used for computing the health index of a given engine, we've chosen to focus on these three winners as they use simpler methods that are easier to reproduce and have been commonly used in more papers.

In first place was T. Wang [5] using a similarity-based approach for estimating the RUL. This approach would attempt to fit a curve using the data available from the testing set using regression models. Due to the shortage of available history from the testing set, this method instead generates a model for each training unit. They also improve this by using a technique called *operating regime partitioning*, which uses the operating settings to determine the operating conditions and preprocess accordingly. They also focused on specific sensors (7, 8, 9, 12, 16, 17, 20) that were chosen as relevant features due to their consistent and continuous trends that can be used for regression and generalization. Wang would later advance this in his 2010 PhD dissertation [6], reviewing different RUL prediction techniques as well as techniques in abstracting trajectory using regression and filters.

In second place was Heimes' Recurrent Neural Network (RNN) approach, which used a set of Recurrent Neural Networks where each calculates the RUL estimation and are then averaged for improved results [3]. Before this, Heimes used an MLP trained with an proprietary Extended Kalman Filter to show the effectiveness of general neural networks. He also introduces a classifier which trains on the first and last 30 of each series of the PHM training dataset, where the first 30 are classified as healthy data points and the last 30 are classified as unhealthy. This was trained with an incredibly high accuracy (99.1%) using a small MLP using only the operating settings and sensors. He then implemented an MLP as a regression-based model, and attempted a basic form of filtering by creating a 'kinked' target function where our target is a constant until below a certain threshold. Although the exact results of the MLP is unknown, using an Ensemble RNN gave Heimes a result of 519.8 for the testing dataset.

In third place, is Peel's MLP and Kalman Filter approach, using an ensemble of MLPs and aggregating using a Kalman Filter [7]. Peel also noticed the operating conditions in the PHM training dataset and the importance of combining the different conditions for predictions. They used a form of data standardization used for each operating condition in order to obtain different features. They would then use an ensemble of MLPs to make the prediction and reduce sensor noise using a Kalman filter after predicting using the ensemble.

This approach has been expanded and further published by others, with expansions on the filter method, preprocessing, and target function [1]. They also described using Root Mean Square Error (RMSE) as the loss function due to it being greater than the scoring function for all  $|d| \leq 30$ . They also showed a way of feature scaling each operating

condition and compared results with a linear target function and kink function. By comparing the linear and kink functions after scaling, they found the kink function performed better when using an ensemble and better optimized the results by using a Kalman filter. They then improved the Kalman Filter by swapping it with a Switching Kalman Filter, giving a significant boost to the ensemble and a much better performance than the standard Kalman Filter.

Table 1

*Results from MLP Ensemble and Kalman Filter Approach [1]*

<b>Methods</b>	<b>PHM Test Scores</b>
Single MLP (Linear)	11838
Single MLP (Kink)	6103.46
KF Ensemble	5590.03
SKF Ensemble	2922.33

## Chapter 2

### Understanding the Data and Experiments

Although we have reviewed our datasets in chapter 1, it is important for us to a deeper understanding our data in order to better analyze and process it for our different models. For this reason, we will be looking into the specific details for each of the datasets, understanding what common traits each has as well as what differentiates them. We will start by looking into the general information for each dataset as well as define the target function used by each of our training sets.

#### 2.1 General Information

Table 2

*Description of NASA Data Repository [2]*

Datasets	# Fault Modes	# Conditions	# Train Units	# Test Units	
C-MAPSS	#1	1	1	100	100
	#2	1	6	260	259
	#3	2	1	100	100
	#4	2	6	249	248
PHM	#5T	1	6	218	218
	#5V	1	6	218	435

As discussed in chapter 1, there are 5 datasets that can be used for this problem (4 C-MAPSS datasets and 1 PHM dataset). Each dataset has a training set and a testing set with different number of engine units, as seen in Table 2. The only exception to this is our PHM dataset which has a final dataset (#5V) used for the original competition. The training set consists of complete runs for each unit, starting from the state of initial use and ending when hitting a failure state. The testing set is similar to our training set, except at some data point our data is cut-off, leaving a partial time series from the beginning with us having to predict based on the last cycle given.

Each time series or *unit* consists of several data points with 26 columns or features. Each of these columns are used to either describe the condition of the engine at the given point in time or to have a reference point for that data point to other data points.

### 1. Unit Number

An integer that defines what series the data point belongs to. This is a fairly anonymous value, meaning we are able to change the unit number for an entire unit without any consequence, so long as it isn't used by any other unit.

### 2. Cycle Number

The time at which this data point describes the engine. The cycle number consists of an integer that increments throughout the series until reaching the final data point,  $n$ .

In simpler terms, cycle number acts as the linear function  $f(x) = x$  within our unit.

This can also be used to define the targeted RUL at a given point for any training set.

### 3. 3 Operating Settings

These 3 columns are used to describe the operating condition of a given data point for a unit. From our datasets, we can have either 1 or 6 operating conditions. More details on operating conditions can be seen in section 2.4.

#### 4. 21 Sensors

These 21 columns define the health of our unit at a given cycle time. Some sensors have more obvious signs of degradation, which is described in chapter 3.

The general structure of a unit can vary from unit to unit and dataset to dataset, but the basic structure can be seen through C-MAPSS 1, which is the simplest dataset in our collection. If we look at Figure 2, we can view our 21 sensors. Most of our sensors begin either at approximately 1 or -1. They begin to curve downward, from positive to negative or negative to positive values depending on each sensor. The main feature of this series is the curving and increase or decrease of value for each sensor, which acts as the degradation of our engine over time.

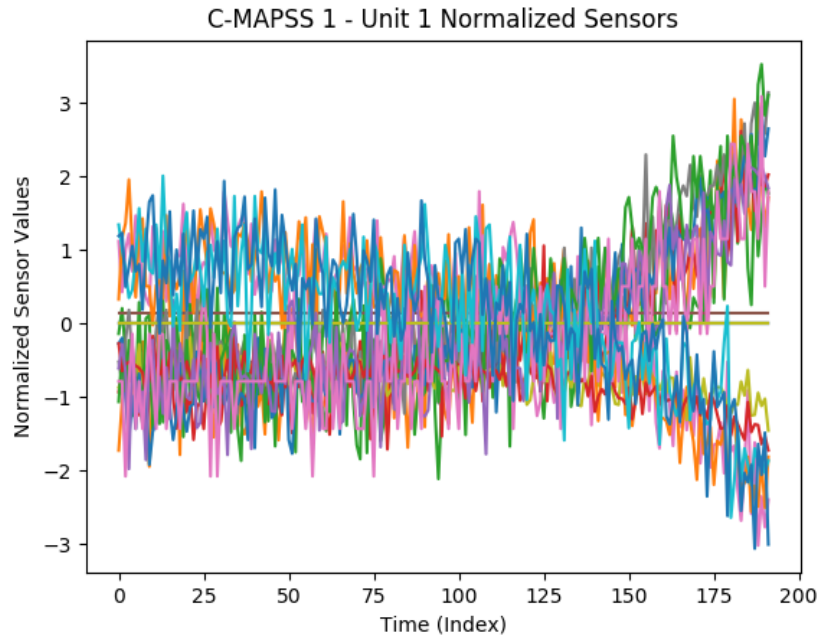


*Figure 2. C-MAPSS 1 - Unit 1 Sensors Example  
(Expanded Normalization from chapter 3)*

## 2.2 RUL Target Function

According to the original PHM '08 Prognostic Data Challenge, the objective of the competition was to predict the number of operational cycles *after* the last cycle for the partial time series, also known as the RUL [8]. Based on this and the fact that our cycle increases linearly with data point order for each unit (as shown in Figure 3), we should expect our RUL to decrease linearly in relation to the cycle for each data point in each unit.

$$RUL(x) = \begin{cases} c - x & \text{if } x \leq c \\ 0 & \text{o.w.} \end{cases}$$

Where  $x$  is the cycle number of a given data point and  $c$  is the maximum cycle number of a given unit

Figure 5. RUL Equation

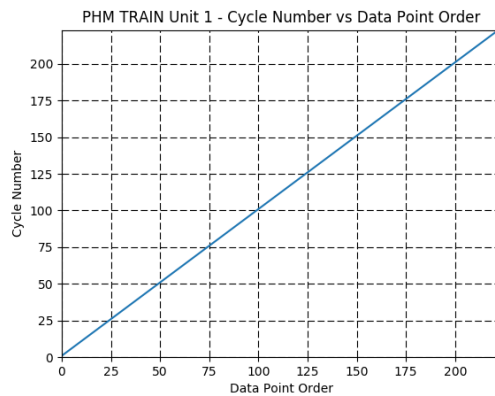


Figure 3. Cycle Number of Data Points in PHM TRAIN Unit 1



Figure 4. RUL Target of Data Points in PHM TRAIN Unit 1

If we understand that each unit has a last cycle, which is also the maximum cycle number, and that our initial cycle number, which is also our minimum cycle number, is 1, then we can simply take the maximum cycle number and subtract it by the cycle number of the given dataset. This can be further simplified by simply reversing the cycle numbers of the given unit and subtract by one, since the cycle number for each unit in the PHM training set increases by 1 for each data point. This true RUL function is shown in Figure 4 and generalized in Figure 5.



## 2.3 Fault Mode

Table 3

*Minimum, Maximum, and Average Length of Series in Datasets*

Datasets	# Fault Modes	# Minimum Length	Maximum	Average
C-MAPSS #1	1	128	362	207
#2	1	128	378	206
#3	2	146	526	248
#4	2	128	544	245
PHM	1	128	357	210

Fault modes are defined with dataset generation, giving us the number of ways our engine may fail. This is based on the physical components defined in the simulation [9]. The effects of fault modes for different datasets has been discussed briefly [6, 10], but not to a large extent in comparison to other datasets.

For each of our training sets seen in Table 3, we find that most of them have a similar minimum series length of 127, with variations on their maximum. However, the datasets with 1 fault mode (C-MAPSS 1, C-MAPSS 2, PHM) have similar maximum lengths less than 400 while our datasets with 2 fault modes (C-MAPSS 3, C-MAPSS 4) have a maximum length greater than 500. This increase of length for C-MAPSS 3 and C-MAPSS 4 is due to their main difference, having two fault modes instead of one.

If we look at C-MAPSS 3, we find that it is very similar to simpler datasets, such



Figure 6. C-MAPSS 3 - Unit 54 (Expanded Normalization from chapter 3)

as C-MAPSS 1 for most units with exception to larger units, such as Unit 54. In those cases, we see more unusual activity from sensors 8 and 13, where a large amount of noise is picked up until normalizing after a period of time. This can be seen in Figure 6, which shows the change of sensor values over time for the given unit. In this case, sensors 8 and 13 are the sensor values below -1 in the first half of the series' life cycle.

We can see more interesting patterns emerge from C-MAPSS 4 after preprocessing it using regime partitioning (discussed in chapter 3). In some units of C-MAPSS 4, we find that it will initially act as a healthy data point, slowly become unhealthy, only to become healthy again and repeat the process one more time. This can be seen in unit 70 of C-MAPSS 4, occurring approximately in the middle of the unit. I am unsure whether this is a product of having 2 fault modes or a part of C-MAPSS 4 itself, but it makes the dataset incredibly difficult to learn. However, this pattern only exists on a few examples seen in C-MAPSS 4, as most units look similar to C-MAPSS 1 in change over time.



*Figure 7. C-MAPSS 4 - Unit 70 (Regime Partitioning from chapter 3)*

From this observation, we can mainly see the difficulty of training datasets with multiple fault modes. This is very obvious in C-MAPSS 4, which has some training series that replicate degradation twice, making our problem much more difficult to solve in these cases.

## 2.4 Operating Conditions

Operating conditions is another feature that changes for each dataset. Unlike fault mode, it doesn't appear to have a great effect on length or any general details we view. However, if we look further into our actual datasets, we find C-MAPSS 1 and 3 look relatively normal, but C-MAPSS 2, 4, and PHM looks as if our sensors are jumping around different points. This can be seen with the PHM dataset in Figure 8. This is troubling as we are unable to have a good understanding of what our data is doing based on these sensors. It mostly looks like noise or some odd transformation.

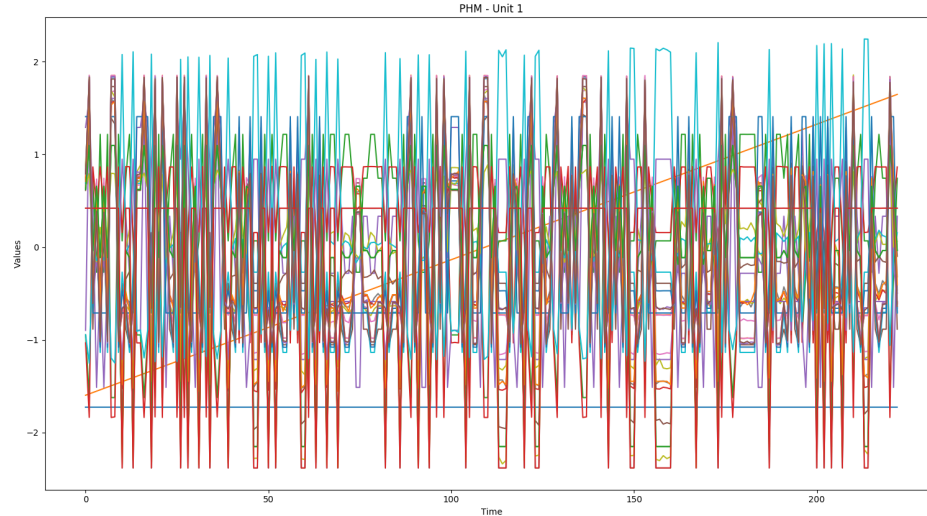


Figure 8. PHM Unit 1 - Expanded Normalization from chapter 3

However, if we try to reduce this into 2 components using *principal component analysis (PCA)*, we find an odd plot forms with 6 clusters, which expands to 7 if reduced after normalizing. We can also see this form similar patterns with each cluster, having a line form from earliest to latest data point. This also mimics the pattern seen when comparing 2 components of C-MAPSS 1 as seen in Figure 9, which only has one operating condition. The reason for this is because each cluster represents an operating condition, with C-MAPSS 1 having only one cluster. These operating conditions have been pre-defined for each dataset, and have also been found independently by several individuals using different methods [2, 3, 5, 10].

This includes the aforementioned PCA method shown in Figure 10, as well as Heimes' method of comparing two signals. For our method, we will be comparing the three operating settings defined in each data point on a 3D grid, which will also give us the 6 clusters for PHM, C-MAPSS 2, and C-MAPSS 4 shown in Figure 11. Using these

clusters, we are able to better preprocess our datasets to give us a better understanding of each unit. This is shown in Figure 7 with C-MAPSS 4, having a more similar projection to our simpler C-MAPSS 1 dataset.

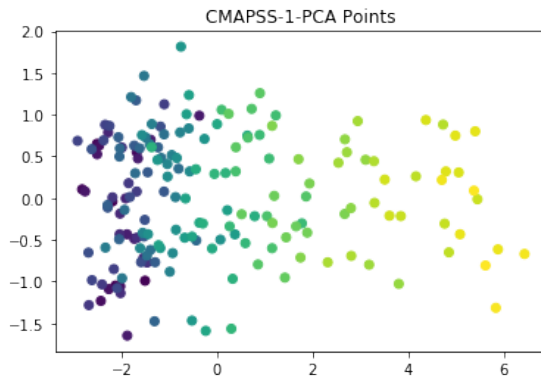


Figure 9. PCA Components of C-MAPSS 1 Train

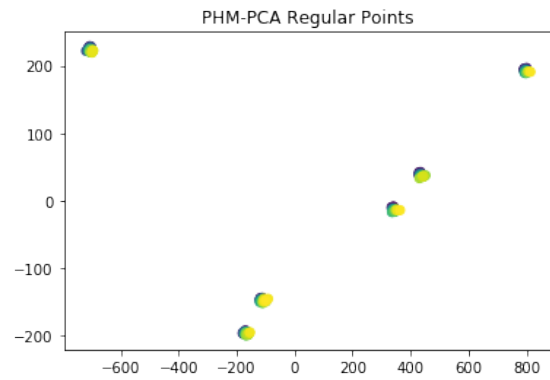


Figure 10. PCA Components of PHM Train

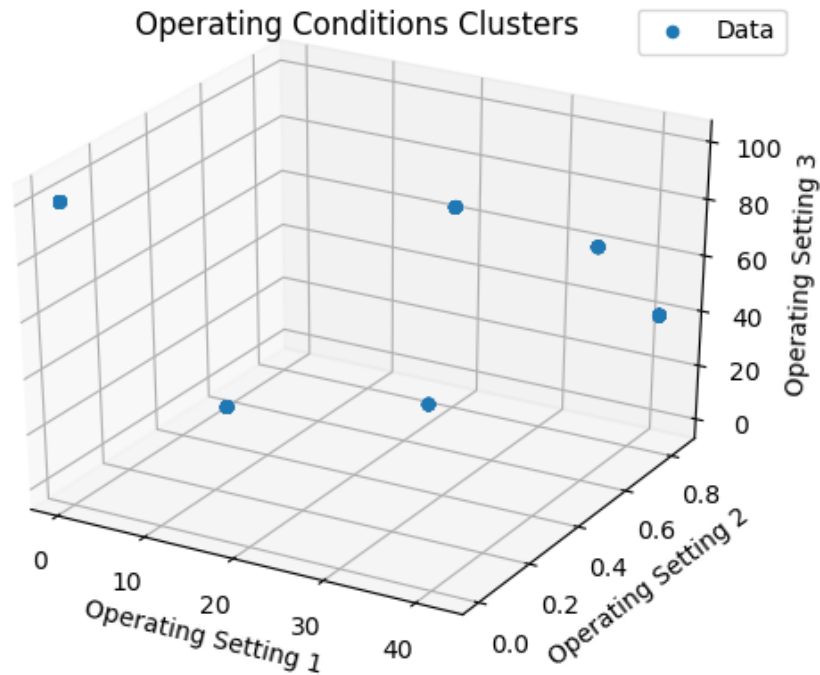


Figure 11. RUL Target of Data Points in PHM TRAIN Unit 1

## 2.5 Testing Data

Table 4

*Minimum and Maximum Length of Series in Test Datasets*

Datasets	# Fault Modes	# Minimum Length	Maximum
C-MAPSS #1	1	31	303
#2	1	21	367
#3	2	38	475
#4	2	19	486
PHM	1	15	367

For general reasons, we don't want to snoop too deeply into our testing dataset as it can give us information that pertains solely to our testing set. However, there is specific information that we should know for when we create our model. If we look into the lengths of our data, we can see in Table 4 that our PHM Testing dataset has the smallest partial length of size 15, giving us a limitation on any batch-based models taking more than one data point at a time. We should also notice that the maximum length of the PHM testing dataset is larger than the maximum length of the PHM training dataset, meaning we may have to make some assumptions or attempt to make our model to go above our maximum length. This will be explored more in later chapters.

## 2.6 Experiment Layout

We will be doing several experiments focusing on the improvement of our score for the PHM testing dataset, primarily through data preprocessing and post-processing. Each experiment focuses on a specific method defined in chapter 3, how it improved our PHM testing score, and a comparison to current methods used. These experiments are:

1. Scaled Target Function: Instead of using our basic target function or common alternative, we propose that scaling our target by some multiplier for training will give us a better score.
2. Cycle Number Inclusion: The cycle number in each data point is commonly excluded in many models. We believe that the inclusion of this cycle number will greatly improve our score since it acts as a referential point of time for each data point.
3. Developing a Classifier Model: Classifications of healthy and unhealthy data points has been discussed and developed in previous papers, but hasn't been commonly used in practice. We believe that a possible model could be made using these classifiers to estimate the RUL.
4. Regime Partitioning versus Expanded Normalization: Two common approaches to data preprocessing is regime partitioning and expanded normalization (standardization). We would like to compare the results for each form of data preprocessing in order to observe their strengths and weaknesses.
5. The Effectiveness of Aggregation and Filtering: Aggregation techniques have been

used successfully with neural network ensembles, primarily the use of Kalman Filters. We wish to implement and reproduce this success using alternative methods, such as other models, curve fitting, and other filters and compare our results with previously used filters.

By doing these experiments, we will be able to have a better understanding on our data and how well different techniques can adjust our data to improve our model for estimation. Each of these experiments also has a focused hypothesis, a defined methodology for how we conducted the experiment, and the result that gives us insight and compares the results or scores of other models.

**2.6.1 Model layout.** We must also have an understanding of what models we are using in order to better comprehend our expected output and for the replication of our experiments. We primarily focused on the use of *feedforward neural networks (FNN)*, also known as a *multi-layer perceptron (MLP)*. Our secondary model used in some experiments was a *support vector machine (SVM)* as well as other baseline models defined in our experimentation.

We also used a *validation set* consisting of a portion of our training set (30% testing/70% training split) to check for over-fitting of our training set. Our final model for submission used all of our data from training. We can see the specifics for our FNN listed below.

(a) Gradient Descent Optimizer: We primarily used *Mini-Batch Stochastic Gradient Descent* with a batch-size of 10 and at most 200 epochs. An Adam optimizer can be used, normally with an epoch of about 80 without over-fitting.



- (b) Activation Function: Our final model uses an ReLU activation function [11], but earlier models experimented with logistic regression activation functions such as sigmoid ( $\sigma(x) = \frac{1}{1+e^{-x}}$ ) and  $\tanh(x)$ . These are defined in our experimentation.
- (c) Loss Function: We chose to use Mean-Squared Error (MSE) as our loss function.
- (d) Layer Dimensions: Generally, each layer size was the same size, default size being 13, with the output being 1. We generally used 1-2 layers for each network as the addition of a third layer didn't seem to improve results.
- (e) Specialized Layers: We attempted to use specialized layers such as Dropout [12], which thinned neural network layers by randomly deciding which nodes in a layer to not use during training. Although this did improve some of our basic models, it didn't seem to improve later models being used.

For our SVM, the parameters are defined with each experiment, with exception to our SMO SVM which is generated via Matlab and uses a Box Constraint array for our soft-margin.

## Chapter 3

### Data and Target Function Processing

Although we may have an understanding our dataset, it would be improper to simply plug in our data into any given model without processing it. As is typical in data analytics, the processing technique used depends on the data. We can focus our preprocessing on specific data columns, such as specific sensors, operating settings, or cycle number. This also includes higher-level properties that are defined by our data such as the operating conditions and fault modes. We may also post-process our resulting output from our model in order to better remove any noise or to correlate the previous input to the current input of the series. We may also find that different target function from the advised target function could lead to better results or improved training of our model.

In this section, we will be discussing methods for processing our datasets as well as their possible advantages and disadvantages compared to other methods. These methods will then be used in each of our different models to evaluate their performance.

#### 3.1 Overview

Broadly speaking, there are five categories of processing methods.

1. *Basic normalization*: These basic forms of preprocessing are commonly used in various forms of data and is not necessarily pertaining to our data. This includes scaling our data, denoising, and standardization.
2. *Regime partitioning*: Modifications between datasets such as the number of operating conditions and fault modes can greatly affect the performance for specific dataset

models, especially as they become more complex. We may see better performance if we tried simplifying these properties by adjusting our data.

3. *Data Selection:* It is common to ignore some variables in a data vector in order to remove unnecessary noise, processing of our model, or to simplify our series. These choices are obviously dependent on the developer, as they can choose to remove specific sensors in each unit depending on its purpose and general display of usefulness in modeling.
4. *Filtering/Aggregating:* Within all of our datasets, there is some form of noise that exists, making it more difficult for us to pinpoint the exact RUL for a given data point. This is also true for our output from most of our given models. A simple solution for this would be to aggregate or filter either our input before training our model, our model's output before submission, or both.
5. *Target function transformations:* Instead of using our target function defined in section 2.2, we may manipulation our target function to receive a better performance from our model.

It is common for most developers to choose between some form of basic normalization and regime partitioning; it is also typical to remove specific data that may or may not benefit our data. We will be focusing on the specific details and differences used by developers and study how they will perform. There has also been brief discussion of using dimension reduction on our data which will be explored in later chapters.

### 3.2 Basic Normalization

When using any dataset, we are able to do basic transformations on our data points using general knowledge of our training set. These techniques, although simplistic, helps us expand to data outside of our training set and help better fit our data so that our model may understand it. This adjustment of values in our data is commonly referred to as *normalization*.

When normalizing, it is common to put our data in a normal distribution based on our known dataset. This is useful as it not only centers our data to our origin, but also treats each our data points equally. This can be done through a process called *standardization*, where any data matrix  $X$  can be computed to the normalized  $X'$  using the following equation:

$$X' = \frac{X - \mu}{\sigma}$$

Where  $\mu$  is the mean

and  $\sigma$  is the standard deviation

*Figure 12.* Standardization

However, standardization doesn't set a distinct minimum and maximum between all of our points. Instead, it simply scales down our data based on all of our values. It may be important to set a strong minimum and maximum for our data in order to better fit a model. Common examples are ranges of  $[0, 1]$  and  $[-1, 1]$  which a model can use to either

set stronger thresholds or to keep a consistent range between all values. This bounding of data between a minimum and maximum is commonly known as *feature scaling* and is computed as follows:

$$X' = \frac{X - X_{min}}{X_{max} - X_{min}}$$

Where  $X_{min}$  is the global minimum  
and  $X_{max}$  is the global maximum

*Figure 13. Feature Scaling*

When using these formulas on our function, we can immediately see an issue with each of our data values as our sensors and operating conditions are expressed in different magnitudes, as shown in Figure 16. This means our global data features (mean, standard deviation, minimum, and maximum) might not properly represent each sensor.

To better incorporate this, we may instead obtain the global data features for each corresponding column to obtain a data feature vector that can be used to normalize each column. This is shown in Figure 14 and Figure 15, where  $f$  is the given column vector.

$$X'^{(f)} = \frac{X^{(f)} - \mu^{(f)}}{\sigma^{(f)}}$$

*Figure 14. Expanded Standardization*

$$X'^{(f)} = \frac{X^{(f)} - X_{min}^{(f)}}{X_{max}^{(f)} - X_{min}^{(f)}}$$

*Figure 15. Expanded Feature Scaling*

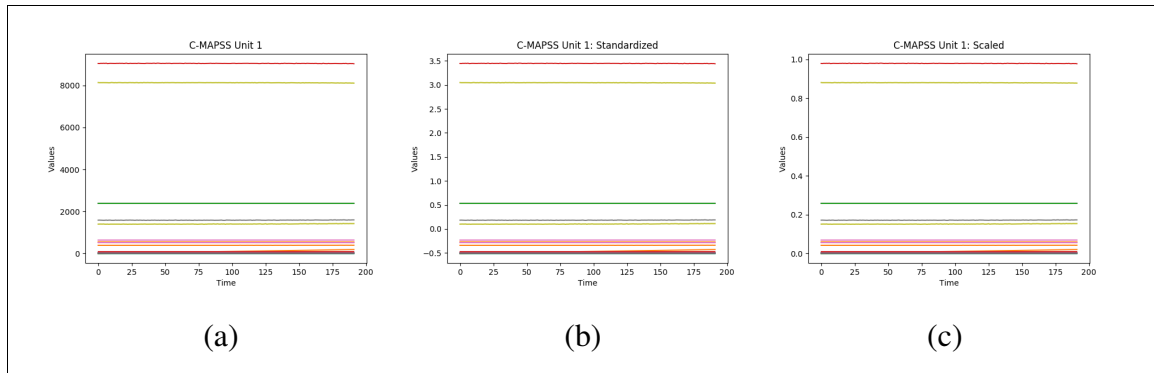


*Figure 16. Normalization Comparison*  
 (a) Original (b) Standardization (c) Feature Scaling

As we can see in Figure 17 and Figure 18, our data is much easier to understand and has a stronger correlation between different sensors, removing the margins giving larger separations between our sensors.

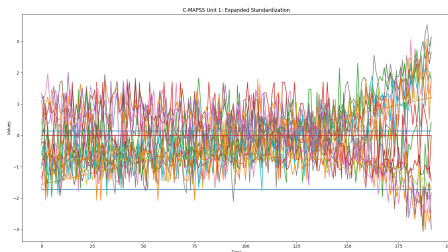


*Figure 17. Expanded Normal C-MAPSS 1*



*Figure 18. Expanded Scaled C-MAPSS 1 [-1, 1]*

### 3.3 Regime Partitioning

The basic forms of normalization work well for simple datasets such as C-MAPSS 1 and 3, but when we attempt the same transformation on PHM we can see a much noisier plot being formed, as shown in Figure 19. As discussed in chapter 2, these unusual data columns are formed by the operating conditions predefined in each dataset. These operating

conditions transform our dataset, making our sensors jump between different operating conditions.

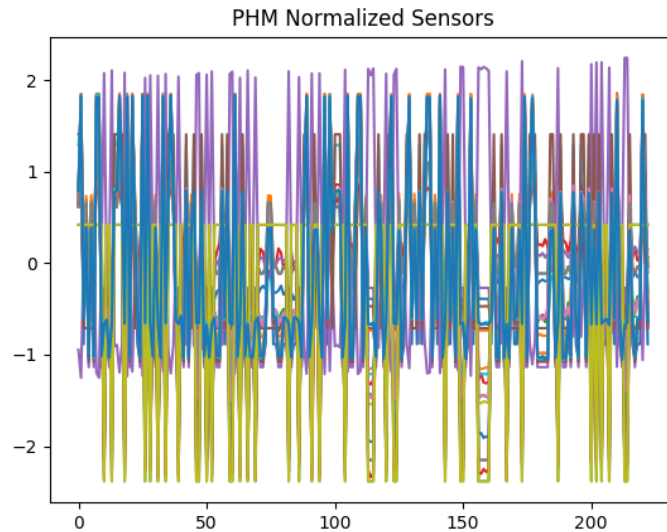


Figure 19. Original PHM Train

As discussed, these operating conditions can be generated using numerous methods that shows the actual linear or exponential patterns shown within each of our sensors. For our purposes, we will be generating the operating condition clusters using the 3 operating settings discussed in chapter 2 and shown in Figure 11. For the purpose of this paper, we will be referring to these operating condition clusters as *regimes*.

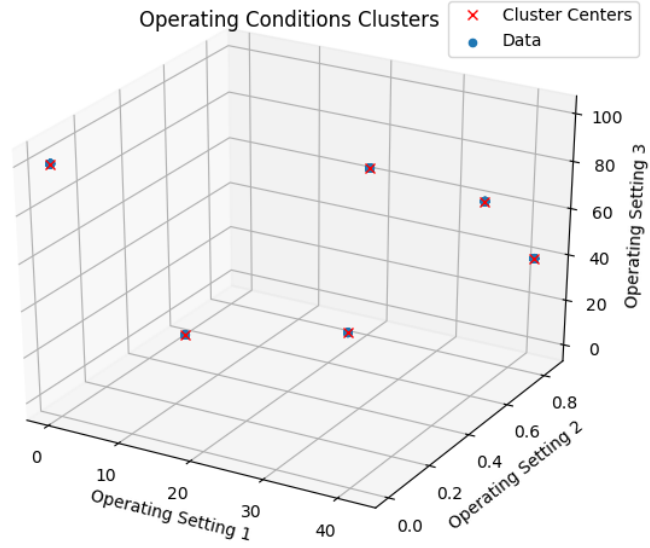


Figure 20. PHM Train Operating Conditions

The operating conditions is shown in Figure 20, but now with cluster centers defined by using K-Means. These centers allow us to classify each point as a separate index from [0, 5]. Using this, we can expand on our previous, expanded normalization process. Instead of simply normalizing each data column, we can instead split each data vector based on our cluster classification,  $c$ , and then normalize each column in each cluster separately. By doing this, our operating conditions will be centered, giving us a relation similar to a single operating condition dataset. This process, also knoww as *regime partitioning*, is generalized for standardization and feature scaling in Figure 21 and Figure 22 respectively.

$$X^{l(c,f)} = \frac{X^{(c,f)} - \mu^{(c,f)}}{\sigma^{(c,f)}}$$

Figure 21. Regime-Partitioned Standardization

$$X^{l(c,f)} = \frac{X^{(c,f)} - X_{min}^{(c,f)}}{X_{max}^{(c,f)} - X_{min}^{(c,f)}}$$

Figure 22. Regime-Partitioned Feature Scaling



After using regime partitioning, we can see a vast improvement with our results. Specific sensors seen in an dataset with 6 operating conditions, such as our PHM dataset, resemble more of a simpler dataset with one operating condition, such as C-MAPSS 1. This can be seen in Figure 17 and Figure 23. However, some sensors seem to be more useful than others, having sensors with less prominent features or curves that better expresses the deterioration of our engine. Please refer to section 3.4 for more details.

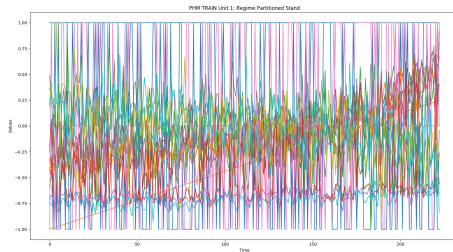


*Figure 23.* Regime-Partitioned Normal PHM Train



*Figure 24.* Regime-Partitioned Scaled PHM Train

**3.3.1 Clustering.** When we know the number of operational conditions, it is easy for us to cluster these operational conditions and perform regime partitioning. The separation can be done in numerous ways, as explained in section 2.4, using multiple signals, our operating settings, Principal Component Analysis, as well as methods of manifold learning. Once we've done this processing, we can cluster our data using K-Means, K-Nearest Neighbor, or some other methods when the number of clusters is known. From this we can proceed this form of normalization.

However, it can become more difficult when the number of operating conditions isn't known, making this method impractical [10]. An easy solution for this is to change the clustering method that can identify some unknown number of clusters. A simple method

for doing this is by using *Affinity Propagation* [13], which generates clusters by sending messages between pairs of point until it converges. It also uses a damping factor,  $\lambda \in [0.5, 1)$  that modifies each iteration by multiplying  $\lambda$  and adding  $1 - \lambda$ .

From doing a small number of experiments using our datasets, we found a damping factor of 0.9 to be effective for finding the correct number of clusters for C-MAPSS 2, 4, and PHM. However, it is more difficult to find the correct number of clusters for C-MAPSS 1 and 3, which have only one cluster. To solve this, you may incrementing the damping factor via magnitudes (increment by 0.1 til fail, increment by 0.01 til fail, etc.) for a set number of iterations. If you find that each iteration of using affinity propagation slowly lowers the number of defined clusers, or there is no set number of clusters for n iterations, then it is expected to be a single cluster.

We didn't perform any major experiments on this methodology as it wasn't the focus of our research, but we found it to be effective with our pre-defined datasets. More experimentation should with a variety of operating conditions and fault modes to ensure effectiveness.

**3.3.2 Purpose.** The generalization of regime partitioning was discussed by T. Wang [6], and has been used for several different models, such as MLP ensembles [1] and expanding on Wang's original works with trajectory-based similarity prediction [10]. It is commonly used for simplifying our model, as seen with our comparison of Figure 17, Figure 23, and our expanded normalized PHM sensors in Figure 19.

However, his method of normalization is mainly viewed in the simplification of individual models and not much has been studied about the transferability of this method to other datasets. We explore this in our experimentation and results.

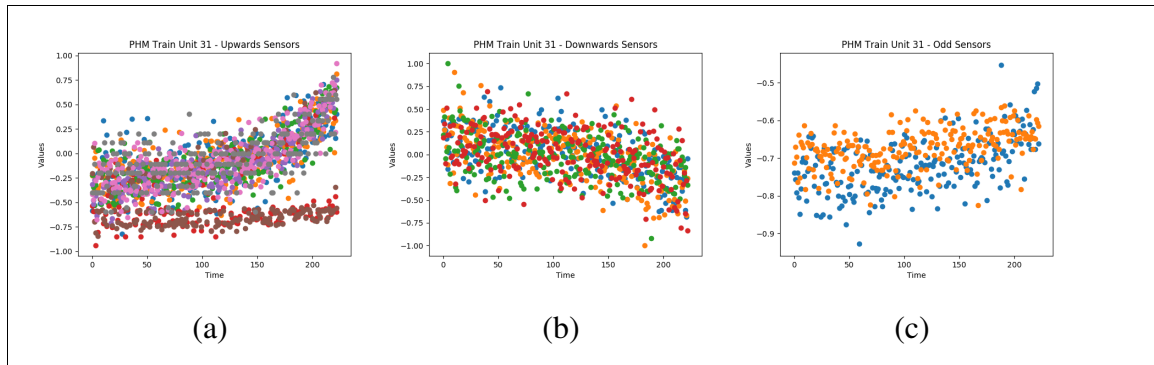


Figure 25. PHM Train - Unit 1 Sensors

(a) Upwards {2,3,4,8,11,13,15,18} (b) Downwards {7,12,20,21} (c) Shifting {9,14}

**3.3.3 Issues.** Some issues with using this approach is that some data columns become unusable due to *nil* values. This includes our operating settings, which are constants in each cluster. Because of the effects of standardization, each cluster is centered, making each constant 0, and then divided by the standard deviation which is also 0. This also occurs with sensors 5, 22, and 23, making them unusable for most situations.

### 3.4 Data Selection

As we saw in Figure 23 and Figure 24, there are sensors that don't seem as important as others, giving us less information and possibly effecting our model in a negative manner. For these cases, it is often important to remove these weak sensors or focus on the stronger features for each of these units.

From our observations of the regime-partitioned PHM dataset shown in Figure 25, we can see interesting trends form in different sensors, usually going upwards, downwards, or either in the case of Figure 25(c). More examples from other units validates these findings, as well as observations of our C-MAPSS 1 dataset shown in Figure 26.

This analysis has also been done by in other studies, focusing instead on seven

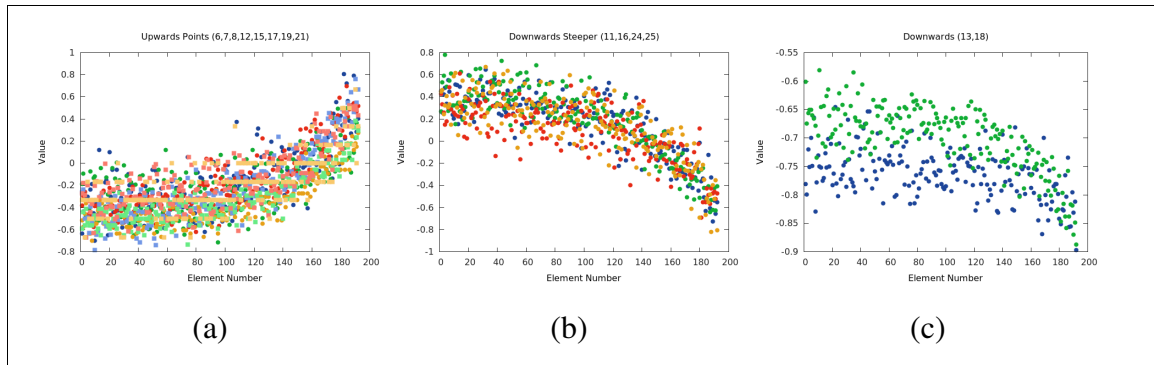


*Figure 26. C-MAPSS 1 Train - Unit 1 Sensors*  
 (a) Upwards {2,3,4,8,11,13,15,18} (b) Downwards {7,12,20,21} (c) Shifting {9,14}

sensors (2, 3, 4, 7, 11, 12, 15) instead of these groupings that we've discussed [2, 5]. A possible reason for choosing these seven is to avoid the splitting that is seen in Figure 25(a) with sensors 8 and 13, and also to focus more on sensors that are more continuously giving us clean results.

Another commonly avoided column for each of our data vectors are the unit number and cycle number defined for each unit. Although the unit number should be avoided since the engines are defined anonymously (as in unit numbers can be swapped without consequence), our cycle number is a set point of time for each data point and cannot be swapped between data points within our dataset, or within individual series. The cycle number is normally substituted in for comparing larger sets of the series, such as the use of recurrent neural networks or similarity-based approaches, but we wish to use the cycle number directly in order to have our model have a more direct component of time.

### 3.5 Filtering and Aggregation

We can see in Figure 25(b) that there is some amount of noise in each of our sensors. In practice, this is also true for the output of our model when input said noisy data, resulting

in a noisy output. A simple fix for this the use of a filter that can adjust our sensors or output for said noise, giving us a cleaner result. This has been described thoroughly in several different papers [1, 6, 9], but we would like to view the different filters that are commonly used and what we believe are also excellent filters for this problem.

**3.5.1 Regression.** An obvious choice would to simply fit a line or non-linear curve onto our given signal. For sensor data, a well fitting curve would be an exponential curve [6] based on the following equation:

$$z = a * e^{b*t} + c$$

where  $a$ ,  $b$ , and  $c$  are the learned parameters,  $t$  is the index (or cycle number), and  $z$  is our new output fitted to the sensor input  $x$  of index  $t$ .

For outputted data that is based on our linear target, we suggest using a 3rd order polynomial curve defined as:

$$z = a*t^3 + b*t^2 + c*t + d$$

where  $a$ ,  $b$ ,  $c$ , and  $d$  are learned parameters. This can clearly vary depending on models, but we found it to be a good fit for our defined models and should cover outputs similar to what was shown by Heimes [3]. In this case,  $z$  is the new output for the original RUL output of a model.

However, this only works when give the full or a large percent of data for a given unit, making this inefficient when given small, partial series such as what is used in our

testing series. For these cases, we would suggest using a linear model defined as:

$$z = a * t + b$$

This linear regression acts similar to our previous two regression models. For our experiments, we use this linear model when the length of the series is less than 30.

The use of fitted regression algorithms gives us a perfectly smooth output, which can be a problem for if we assume too much of our data is noise. For this reason, the use of actual filters may give better performances, keeping more of our noise in order to keep more of our actual data.

**3.5.2 Kalman filters.** A filter that is commonly used in not only this problem [1, 6] as well as several others is the Kalman Filter. Several different Kalman Filters have been used with great success, but also with large amount of variance. To avoid focusing on a single class of filters, we decided to make a simple Kalman filter based on Welch and Bishop's introductory paper [14].

**3.5.3 Butterworth filter.** The Butterworth filter is a relatively simple, but effective filter that uses two coefficients in a forward-backward filter [15]. This gives us a very smooth output after filtering similar to our Kalman filter. However, we do see more curves near the end of some partial series, giving a possible over-estimation of our data. To avoid this, we change the order for our butterworth coefficients from 3 to 1 when the length is less than 30, similar to our regression models.

**3.5.4 Savitzky-Golay filter.** Many of our previous filters focuses on giving us a fairly smooth output after filter. However, focusing on smoothing the connections from one

point to another leads to possible over-curving of data and a poor estimation. Furthermore, a focus on our entire, noisy series can lead to other poor estimations. For this reason, the Savitzky-Golay filter is an excellent alternative to our previously defined filters [16]. Unlike many of our other filters, it focuses on a "window" of adjacent points and fits it to a low-degree polynomial. For our experiments, these windows would use a third of the total length of the series, but would be capped at 33 if they were too large. Similar to our regressions models and butterworth, our order was set to 3 if the length was greater than 30, else it was set to 1.

### 3.6 Target Function Transformations

Instead of using our basic, linear target function that we discussed in section 2.2, we can instead train on an alternative target function based on some assumption of our data. This can help improve our model's performance while having minimum loss for our true target. There is one method that is commonly used, the kinked function, and our method of scaling down our target function.

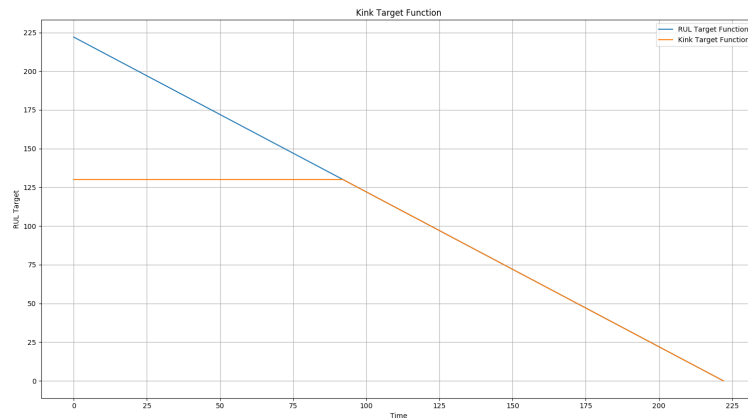


Figure 27. PHM Train - Unit 1 Kinked Target Function

$$Kink(x) = \begin{cases} 130 & \text{if } x \geq 130 \\ x & \text{otherwise} \end{cases}$$

Where  $x$  is the computed RUL for a training unit.

*Figure 28. Kinked Equation*

**3.6.1 Kinked function.** The kinked function is a commonly used target function defined originally developed by Heimes for the original 2008 competition [3], and has been used to improve more recent methods as well [1]. It originates from the idea that the lowest run length is 128 (127 if starting at 0), and having the later, unhealthy portions of our series defining the actual RUL. This means we can instead focus less on the healthier portions of our series and focus more on the later, more defining features.

By taking this into account, we can define a target function take has our RUL defined as 130 if our linear RUL is normally greater than or equal to 130, and is otherwise the linear function itself. This is visualized in Figure 27 and is formalized as:

However, this function may over-assume parts of our testing set which only contains healthy states. For instance, in our PHM testing dataset, we have a unit that is of length 15. Because all of our series start healthy, we know that a good portion of these data points might be healthy and default to 130, giving a possible worse estimate.

**3.6.2 Scaled target function.** Instead of adding a kink to our target function, we can instead keep our target linear, but scale down our targeted output instead. This can be done by looking at the maximum RUL of our given dataset and dividing our original RUL



by that maximum, giving us a scale from 0 to 1. This is typically done for converting our regression model of  $[0, \infty]$  to a logistic regression model of  $[0, 1]$ . After training, we can input our testing dataset to our model and multiply by the maximum RUL, also referred to as the *max-multiplier* of our model. Doing this may help in simplify our learning and also make a clearer assumption about the expected length for a dataset.



Figure 29. PHM Train - Unit 1 Scaled Target Function

This can also be expanded to scaling our model from  $[-1, 1]$  by then multiplying our  $[0, 1]$  target by 2 and subtracting by one. Any expansion can be described using the feature scaling algorithm. For our purposes, we will be focusing on simply scaling down our target function to  $[0, 1]$ . This can be seen in Figure 29 which scaled the first unit of our PHM training dataset by the max RUL, 356.

## Chapter 4

### Experiments

We can see from chapter 3 that there different methods of preprocessing and post-processing data, as well as the different available target function for our model to train on. To further understand these methods require a breadth-first search for us to see their general effectiveness, as well decided on more general methods and combinations of methods in order to optimize our results. This is reflective of our experiments, defined in section 2.6. In this chapter, we are showing our hypothesis, methodology, and results for each experiment as we approach a better model.

As previously stated in chapter 1, we have a score function (Figure 1) that increases as when RUL estimation is over or under the exact amount. The score function also gives a heavier penalty for over-estimations than under-estimations. For instance, an overestimation of 60 leads to a score increase greater than 400, while an underestimation of 60 leads to a score increase of approximately 100.

#### 4.1 Baseline Models

Early on we chose to use feedforward neural networks (FNNs) due to familiarity and existing libraries that heavily support it (primarily Tensorflow and Torch). In order to confirm our results with our FNN model, we decided to create several baselines for when we heavily modify our FNN model. We preprocessed our data using expanded standardization, a very simple form of preprocessing that would keep our data in a simple range. Using this, we generated several different models with a basic target function and used this as our starting baseline. The score would be based on our submitted PHM testing dataset.

Table 5

*Baseline Models Comparisons*

Model	PHM TEST Score
Linear SVM	23,509.33
SMO SVM	24,060.66
Ensemble	482,740.00
Gaussian	2,363,057.25
Decision Tree	1,288,502,988.08

**4.1.1 Results.** From these results in Table 5, we get an understanding that the linear model is the best model followed by our SMO SVM, and our other models are fairly weak. This could also be due to the difficulty of the problem, where our linear model is performing the best based on its simplicity. If we were to submit an RUL of 54 for all 218 units in our PHM testing dataset, we would find this aligns with this conclusion as this constant gives us a score of 24,505.19, only slightly worse than our SMO SVM.

We can take 2 major points from these results:

1. Our model should be relatively simple to achieve better results.
2. Scores of 20,000 or greater are weak predictors.

The first point is fairly obvious and follows Occam's razor. However, the second point tells us what models gives us an insight to the unit series and what models tell us little or nothing. We may possibly assume that the average of this constant RUL score may give us

insight to other datasets as well for comparing results ( $\frac{24,505.19}{218} = 112.41$ ).

## 4.2 Max-Multiplier Experiment

The use of FNNs is fairly common for this problem and has been done several times using the basic target function. The kinked function was also defined in several papers and in practice [1], leaving us to more thoroughly investigate the idea of scaling the target function using a multiplier.

**4.2.1 Hypothesis.** We didn't believe that this form of optimization would lead to any absolute failures and believed that, at worst, it could slightly lower the score of good models. For this reason we wanted to focus on creating what we considered the best model using this method and compare to see whether it actually improved our model.

As for actual improvements, our hypothesis is that scaling down our data would improve our model results and aid in the training of our model, or at worst do nothing to our data. We will be focusing more on this hypothesis in our comparison.

**4.2.2 Methodology.** We used an initial FNN (24x5x3x1) similar to what was described by Heimes [3]. If you notice, we are only taking 24 inputs, meaning we are excluding our cycle number and unit number from our input. Our initial activation function were sigmoids ( $\sigma(x) = \frac{1}{1+e^{-x}}$ ) since our data was scaled from 0 to 1, making our neural network estimator for the RUL take a logistic regression approach. We then attempted to scale up this model in order to achieve better results.

Table 6

*Initial Neural Network Comparisons*

Model	PHM TEST Score
24x5x3x1	47,457.67
24x13x13x1	31,746.61
24x13x13x1 w/ 1st Layer Dropout	18,892.87

**4.2.3 Results.** Initially, our neural network did incredibly poorly, scoring worse than our linear model and our constant RUL. We then tried to improve our model using adding another hidden layer, which improved our score by over 10,000, giving us a new score of 31,746.61. However, we shouldn't consider this a victory since it is still worse than our baseline score. The biggest improvement was the use of Dropout [12] with a 50% probability of cutting an output from our first layer. By adding this one change our score was cut by almost half, and more importantly, putting us below our baseline.

We can also compare the results of our first and second best models from Table 6 by graphing a unit series from a validation set. If we observe Figure 30 and Figure 31, we see our Dropout model, which performs better than our non-Dropout model, has a larger amount of noise generally seen with each unit in our validation set. We would expect the opposite to occur based on our scores, but based on the figures we assume visualizations of these output are inaccurate, at least until we achieve better results.

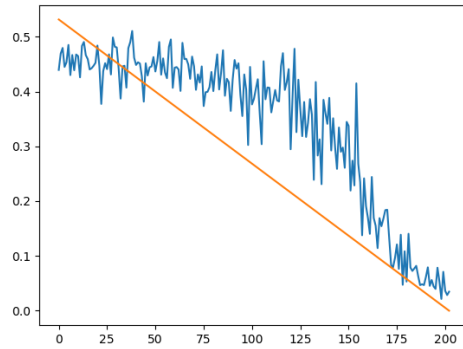


Figure 30. PHM Train Validation Set (24x13x13x1)

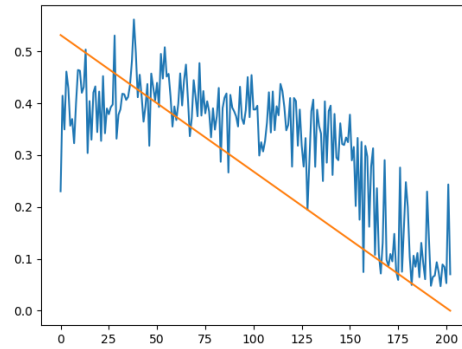


Figure 31. PHM Train Validation Set (24x13x13x1 - Dropout)

After running these models we attempted to improve our model using similar methods, but with no success. This concluded our experimentation with our max-multiplier, as we decided to focus on other experiments.

### 4.3 Cycle Number Inclusion Experiment

Currently, most models exclude the cycle number of a given data point to instead use some form of aggregation or continuation such as recurrent neural networks to chain data points together. Instead, we chose to keep our model simple by using our basic FNN and including this cycle number as part of our data.

**4.3.1 Hypothesis.** Our hypothesis is that the inclusion of the cycle number will improve the results dramatically as well as improving our structure of our output. This belief comes from how our RUL itself comes from our cycle number and giving our models a comparative stance between different data points.

**4.3.2 Methodology.** To show this, we generated two similar models based on our current best model defined in Table 6. In this case, we use the same model with 24 inputs and another model with 25 inputs. We also updated our activation function to use ReLU

[11] for easier experimentation with later examples. This change of activation function still keeps our score relatively the same.

Table 7

*Cycle Number Inclusion vs. Exclusion*

Model	PHM TEST Score
Without Cycle Number	18,892.87
With Cycle Number	9,946.4

**4.3.3 Results.** We found the results after using the cycle number to be staggering. Once again, our score has been cut in half, giving us a much better model for us to work with. Another staggering result comes from removing the Dropout layer, cutting our score by more than a third with a result of 3,285.91. Because of this, our best model removes Dropout, giving us a 25x13x13x1 FNN with ReLU activation functions.

When comparing this current model with other scores, we found that it outperformed methods using the basic linear target function and kink target function [1]. We were also able to replicate these scores for each target function and found our reasoning to be sound.

#### 4.4 Classifiers Exploration

We decided to attempt another approach in estimating the RUL for each series based on other methods. In Heimes' paper [3] he experimented with a basic classifier, classifying the first 30 of each unit in our PHM training set as healthy and the last 30 as unhealthy.

Using this data, he found it was easy to train a basic FNN model.

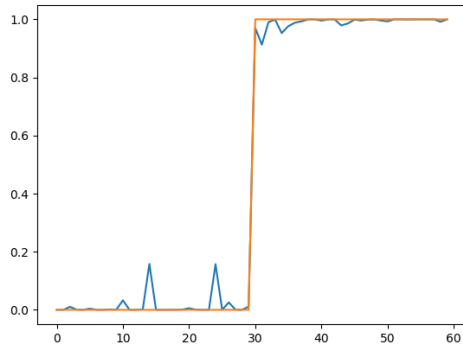


Figure 32. Accurate PHM Train Unit FNN Classifier

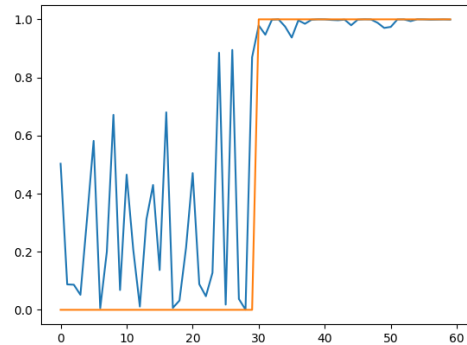


Figure 33. Inaccurate PHM Train Unit FNN Classifier

When replicating, we found it to be fairly accurate, but with some issues with our validation set. This can be seen in Figure 32 and Figure 33. The use of an SVM Classifier can improve this, but assumes our data is absolute 0 and 1, as shown in Figure 34 and Figure 35.

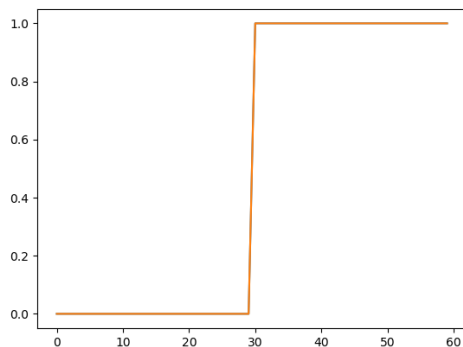


Figure 34. Accurate PHM Train Unit (100% Accuracy) SVC

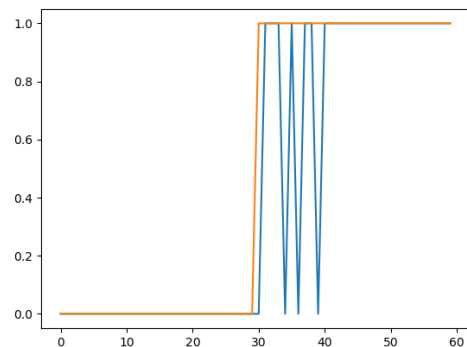
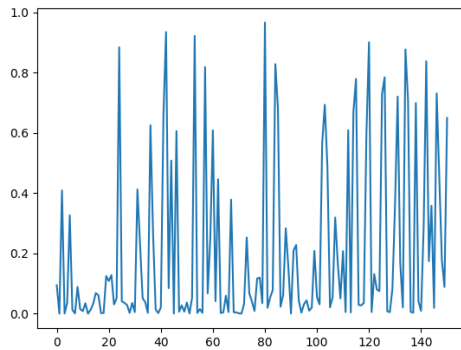


Figure 35. Inaccurate PHM Train Unit SVC

However, when using our models to predict the PHM testing dataset we found that it didn't seem to make any accurate predictions, as shown in Figure 36. We then built similar



models, but using the cycle number as an additional input. By doing this, we saw clear patterns of transitions from 0 (healthy) to 1 (unhealthy) in larger test series. This trend is shown in Figure 37. Although we can't make an accurate score because of this being our test set, we can believe that the inclusion of this cycle number improved our results due to the expected trend.



*Figure 36.* PHM Test Unit  
FNN - No Cycle

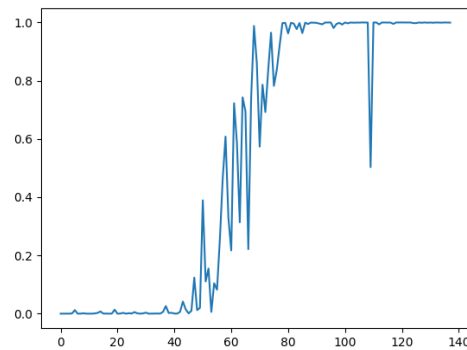


*Figure 37.* PHM Test Unit  
FNN - Cycle

**4.4.1 Hypothesis.** Using these classifiers, we may create a new way of generating the RUL estimation for each PHM test series. Our hope is that this method will achieve better results than our aforementioned score of 3,000.

**4.4.2 Methodology.** Our first thought was to split our data further instead of simply using the first and last 30 for each series. To do this, we took each series and split them into 5 buckets containing 20% of the series. We then generated 4 classifiers, each splitting the buckets so that  $N$  buckets represent the data points below  $(N * 20)\%$  of the series, classified the 0. The rest are then classified as 1, representing being above our split point. Each model would consist of either the use of SVC or a FNN that consisting of the same hyper-parameters defined with our results.

After generating each classifier, we then split our classification by taking a average of a window throughout the series until we reach an average  $\geq 0.5$ , in this case we chose a window size of 5. We also experimented with how to exclude specific classifiers if given faulty results, such as be given a series size less than the percentage rated by the classifier.

**4.4.3 Results.** As shown in Table 8, an initial use of an SVM finds our results to be poor, doing worse than our linear model and our constant RUL model. We attempted to remedy this by changing the soft-margin for the SVM, and found a middle ground of 100 gave us the best results. However, this didn't line up with our scores for our validation set that found lower penalties gave better results.

Table 8

*SVC Classifier Comparison*

Models	Test Score	Notes
SVC(C=1, degree=3)	22,041,035.27	If RUL < 0, negate
SVC(C=5, degree=3)	2,494,705.23	If RUL < 0, negate
SVC(C=10, degree=3)	1,557,058.77	If RUL < 0, negate
SVC(C=50, degree=3)	761,054.59	If RUL < 0, negate
SVC(C=100, degree=3)	759,380.40	If RUL < 0, negate
SVC(C=500, degree=3)	1,068,366.77	If RUL < 0, negate
SVC(C=1000, degree=3)	1,072,458.20	If RUL < 0, negate

We then changed our model to an FNN using ReLU activation functions and found

our results drastically improved, but not enough to beat our linear model. We also tried to increase the size of our model, which did give us improvements but, we found that our best score was still 10 times more than our baseline models.

Table 9

*FNN Classifier Comparison*

Models	Test Score	Notes
MLPClassifier((32, 24, 16))	525,979.31	results $\leq 0$ become 0
MLPClassifier((32, 24, 16))	297,137.01	results $\leq 0$ are ignored
MLPClassifier((32, 24, 16))	391,050.62	results $\leq 0$ are ignored
MLPClassifier((32, 24, 16))	248,462.45	If output is $< 0$ , negate

We also ran into issues with negations and models classifying the entire partial series the same, making our ensemble more difficult to deal with. We found the best way was to negate these values, which still gave us several issues to deal with. In short, we couldn't find an effective way to use this ensemble.

#### 4.5 Regime Partitioning

After running with expanded normalization, we decided to attempt to improve our model using regime partitioning as our main method for preprocessing. We wanted to attempt to see the advantages to regime partitioning to our current method and if there was any actual advantage for the PHM dataset alone.

After working our experiments with our PHM dataset, we decided to expand our

work to the C-MAPSS dataset to see how our methodologies compare with different, but similar datasets. Although our previous results are valid for PHM, harder datasets may become more difficult to deal with or less complex datasets are easier to deal with. This seems to hold true for other papers that analyzes more than just PHM [1, 10]

**4.5.1 Hypothesis.** We expect regime partitioning to improve the results for our model and making it more relatable to other datasets by simplifying the clustering used for operating conditions.

**4.5.2 Methodology.** We will be using a (25x13x1) model with ReLU activation functions for our expanded normalization and a (19x13x1) model with ReLU activation functions for our regime partitioning. This lowering of inputs is due to the operating settings becoming nil after performing regime partitioning and some nil sensors as well.

We also expanded these experiments for other datasets as well and for models without the use of cycles. We hope that this will give us more insight into the performance of other datasets and how well they fit into our current best model.

Table 10

*Expanded Normalization vs Regime Partitioning*

Preprocessing Method	PHM Test Score
Expanded Normalization	3788.18
Regime Partitioning	7454.48

**4.5.3 Results.** We can see in Table 10 that our hypothesis was wrong for the PHM dataset. Our expanded normalization preprocessing outperforms our regime partitioning method. This is incredibly odd since most people tend to use regime partitioning in some form for the preprocessing [1, 6, 10]. We also confirmed by improving our model, receiving similar results to the first place winner [5].

We should expect regime partitioning to have some advantage over different datasets, especially considering how it reduces the operating conditions for all datasets. For this reason, we decided to continue experimenting using several datasets instead. We also focused on submitting to each testing dataset for each of our datasets in order to see any transferability that could possibly exist.

Comparing Table 11 and Table 12 shows an unusual side that we didn't notice before. Although our cycle number does improve each of our datasets in comparison of not using a cycle number, we find that training on other datasets, in some cases, gives us better performances. This can be seen with training on C-MAPSS 4 and testing on C-MAPSS 2, and larger effect can be seen when training on C-MAPSS 1 and testing on C-MAPSS 3.

Table 11

*Total RUL Score (Expanded Normalization w/ Cycle Number)*

C-MAPSS 1 (100 Units)	2 (259)	3 (100)	4 (248)	PHM (218)
3429.553159	2399917.454	22300.42896	1647158.566	180336.68
4.05867E+23	44638.41142	5.09041E+27	49295.23293	624058.5
68866916.31	3.20382E+17	611805096.2	9.71451E+15	1.24402E+15
3.71893E+34	34429.74452	7.57986E+43	50885.48583	2.85E+12
7.29278E+24	4.84E+13	8.35206E+24	1.02901E+15	3788.18
Best Average Scores Per Unit				
34.29553159	132.9333765	223.0042896	198.7711005	17.37697248

Table 12

*Total RUL Score (Expanded Normalization w/o Cycle Number)*

C-MAPSS 1 (100 Units)	2 (259)	3 (100)	4 (248)	PHM (218)
3803.443683	14824498464	28085.71268	12252365456	305838154026
7.94307E+60	37548.80635	5.74752E+48	273777.7273	15241257.85
84630.96189	5.67E+14	1799097270	4.00E+14	2.73E+16
1.68878E+47	141227.5593	1.29892E+57	125751.2301	7.99E+20
6.84274E+25	4.10664E+17	4.28921E+23	3.99788E+17	19028.79883
Best Average Scores Per Unit				
38.03443683	144.9760863	280.8571268	507.0614119	87.28806802

We also find that PHM is the best performing out of all of these methods, followed by C-MAPSS 1, which has double the average score. Training on more complex model improves C-MAPSS 1 down to an average score of 27.20, but this still doesn't beat our PHM test dataset score.

Table 13

*Total RUL Score (Regime Partitioning w/ Cycle Number)*

C-MAPSS 1 (100 Units)	2 (259)	3 (100)	4 (248)	PHM (218)
3020.925557	168353.4269	640517.8762	11605879.04	9953.780619
4291.80613	43024.96287	6918.228081	85679.14248	6583.142585
33698.13	626170681	1400206201	96972108.7	3975518.175
32251.86555	903563.2456	6734.379265	136110.2005	219623.6999
4121.551745	36958.98043	4343.471254	37361.1906	7454.484125
Best Average Scores Per Unit				
30.20925557	142.6987662	43.43471254	150.6499621	30.19790176



Table 14

*Total RUL Score (Regime Partitioning w/o Cycle Number)*

C-MAPSS 1 (100 Units)	2 (259)	3 (100)	4 (248)	PHM (218)
3795.738041	2351129.624	6011.477993	882622.7645	144126.4734
6575.075802	43700.05936	14441.78701	255942.8523	22050.56435
187766.8253	45561902395	339487646.4	11410625871	6642300.283
5768461.887	1086365.845	36355.79442	171475.16	452604.8415
4937.49241	39277.00515	21200.11688	337992.5004	70942.42205
Best Average Scores Per Unit				
37.95738041	151.6486685	60.11477993	691.4320969	101.1493778

We found that using regime partitioning, the general results for 3 of our 4 C-MAPSS datasets did improve, but still in strange ways. Our best method for training C-MAPSS 3 and C-MAPSS 4 datasets was by training our model on our PHM dataset. Oddly enough, our C-MAPSS 2 dataset didn't improve at all from this transition, as well as our PHM dataset. However, C-MAPSS 1 improvement is self-contained and due to the decrease of inputs.

We can also analyze the relation between these datasets, and although the score didn't improve for some datasets, we do see some score improvements based on relations, as well as an lower total average between scores trained on different datasets. We also

see C-MAPSS 2 giving PHM a better output than training on PHM in this case, similar to our previously described relations with other datasets. This makes regime partitioning a possible improvement for more general datasets, especially when dealing with an engine differing from our training set.

#### **4.6 Aggregation via Filtering**

We found our current best model gives us a score of 3285.91, but this can still be better improved for PHM by using different techniques. In this case, we wish to improve the noise of our current output model by using some method of filtering. This method of filtering has been used before with specialized Kalman filters [1], but we wish to look at simpler methods in order to see what types of filter may work better given specific circumstances.

**4.6.1 Hypothesis.** We believe filtering our output will improve the score of our model by a significant amount, but different methods that could over-smooth our output could cause damage to our score instead.

**4.6.2 Methodology.** We will be using the following methods for filtering the same output for our best model (25x13x13x1 with ReLU activation functions):

1. SVM
2. Random Forest
3. Fitted Curve
4. Butterworth Filter
5. Savitzky-Golay Filter

Each method will then be compared with the original output and the other method used, along with an analysis of their performance compared to their filter. We chose against using the Kalman filter as it was previously done by Lim's team with other specialized Kalman filter that we didn't focus on building due to time constraints. We will be comparing our score difference with theirs as a result.

**4.6.3 Results.** The SVM and Random Forest models were trained by taking the output of our best model as an input and re-training with our target function. Using this method, both models failed in incredible fashion, possibly adding more noise to our output. This can be seen in Figure 38 and Figure 39, which is shown adding more noise or having no effect on our PHM testing dataset. In both cases, the models made our output worst, giving us a score of 4549.81 and 18,558.33 for the SVM and Random Forest respectively.

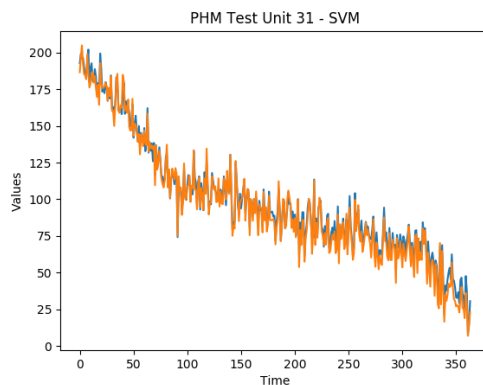


*Figure 38.* PHM Test Unit 31  
SVM Filter

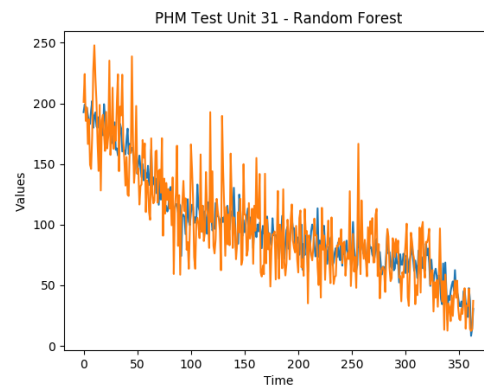


*Figure 39.* PHM Test Unit 31  
Random Forest Filter

However, using the fitted curve described in chapter 3, we can instead fit our outputted series to a 3rd order curve or 1st order line depending on length. Doing this removes the chances of noise and helps us better filter our model. We can see relative success based on the curved line in Figure 40 and Figure 41 that is based on our noisy output. These

figures also show that the polynomial is more centered throughout our noisy output instead of estimating over or under, although there are some curves that go over specific periods of our output series.

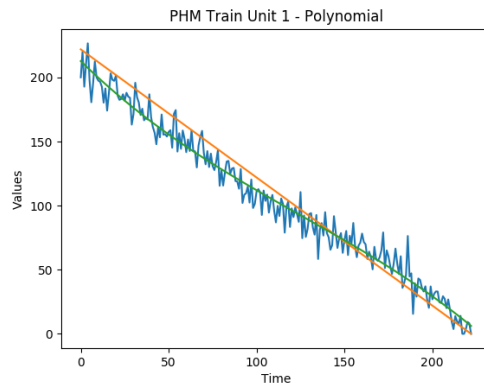


*Figure 40.* PHM Train Unit 1  
Polynomial

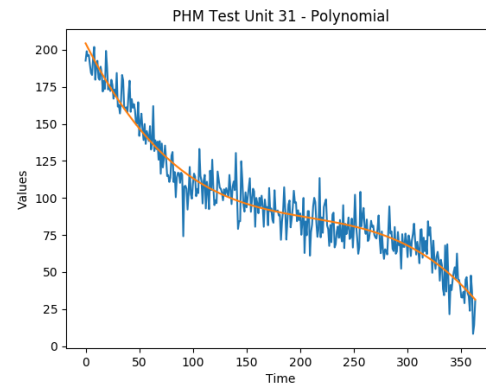


*Figure 41.* PHM Test Unit 31  
Polynomial

By using this polynomial as our new output, we found our results improved from 3285.91 to 2700.20, or a reduction of 17.82%. Although we find this method to be effective, it is possible that we are over-simplifying our model. This can be seen in Figure 42, draws a line within 15 data points. This new output might be overly-centered, as we don't have later data points that give us more information later on to drag our polynomial down. To fix this, we can refer to our actual filters.

Our first filter, the butterworth filter, is a classic filter used for several problems with signals. If we look at Figure 43 and Figure 44, we can see a similar pattern to our polynomial curve fit, but with a better fit to local data. Because of this, we expect a better score for our new output.

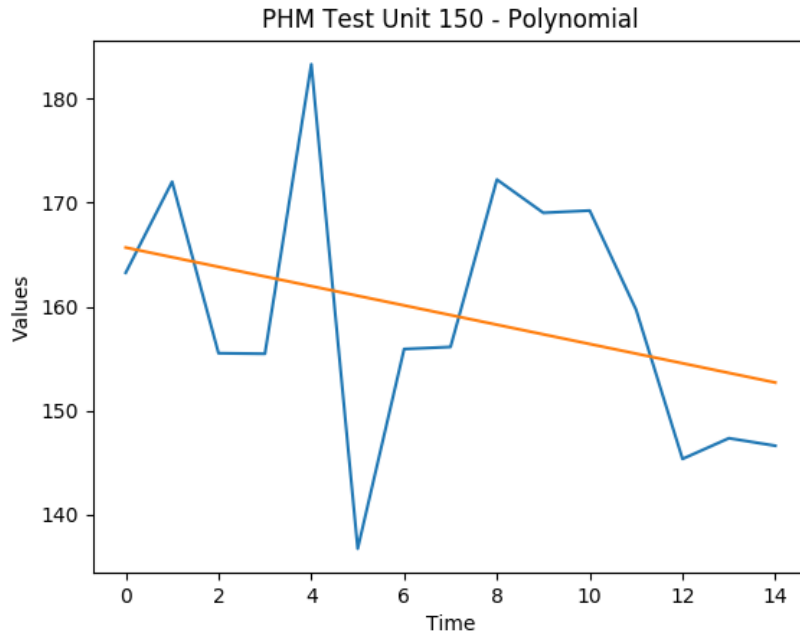


Figure 42. PHM Test Unit 150  
Polynomial

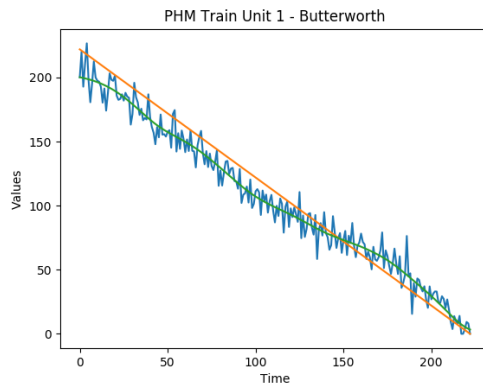


Figure 43. PHM Train Unit 1  
Butterworth

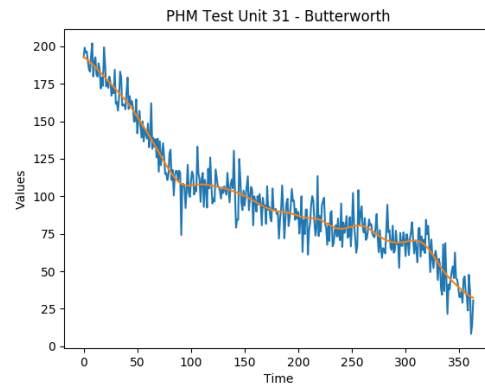


Figure 44. PHM Test Unit 31  
Butterworth

However, we instead find that our results slightly increased to 2739.74, still a major reduction when compared to our PHM dataset. We found this odd, as it looks as if it is better fitting with our data, as seen in Figure 45, however we do see some curving in

the beginning and end of some series, possibly leading to slight over-estimations or under-estimations. Considering that we look at the last value of our series for the RUL estimation, this can become a concern.

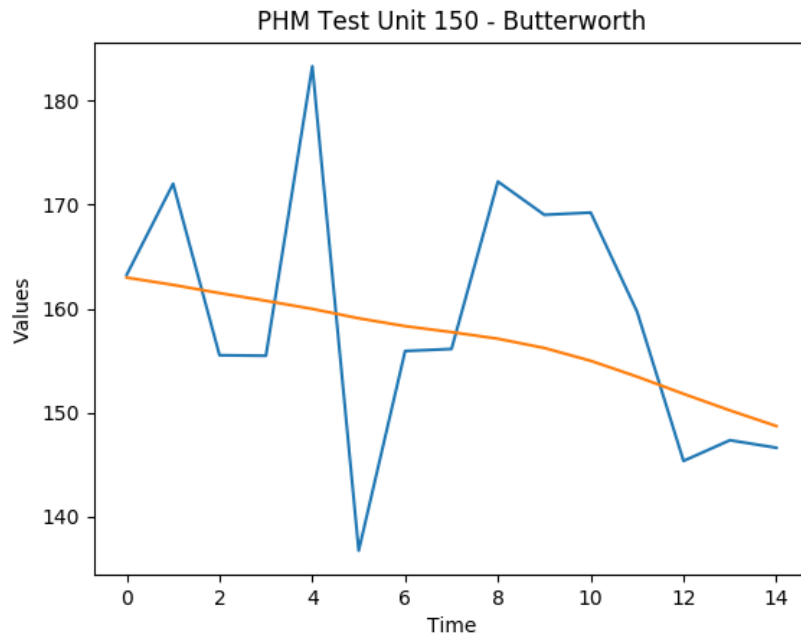


Figure 45. PHM Test Unit 150 Butterworth

Many of these previous filters focus on smoothing, which could lead to some, local oddities within our data. A simple way to this is to use a convolution-based filter with a window so that it can focus solely on a local region instead of the entire data series at whole. This convolution-based filter is also known as the Savitzky-Golay filter, and for our version of this filter we have not only lowered the polynomial order for shorter, partial series, but also varied the window size based on length as well (more details in chapter 3).

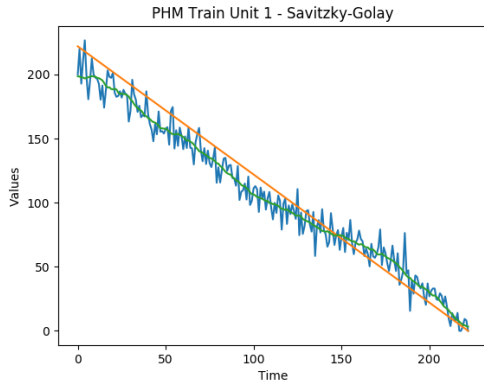


Figure 46. PHM Train Unit 1  
Savitzky-Golay

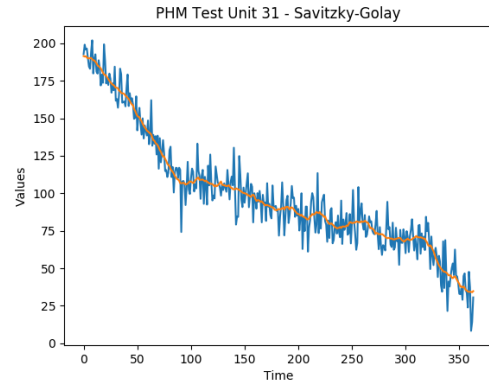


Figure 47. PHM Test Unit 31  
Savitzky-Golay

We can see in Figure 46 and Figure 47 that this filter acts similarly to our Butterworth filter, but with more of what appears to be possible noise. However, by doing this we are under assuming the limits of this noise and keeping more of our original output within our new output.

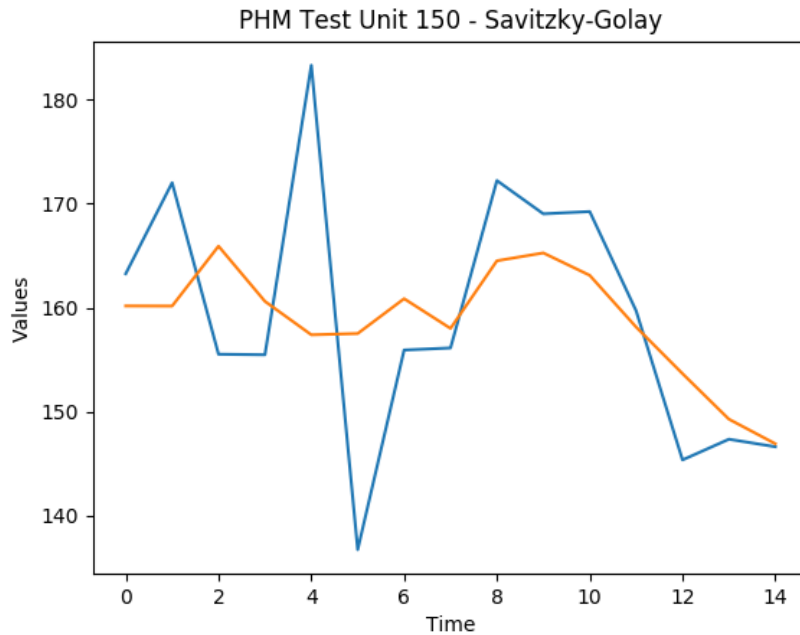


Figure 48. PHM Test Unit 150  
Savitzky-Golay

After submitting the output result of this filter, we can see a tremendous amount of success, as we a score of 2,260.69, reducing our original best model score of 3285.91 by almost a third. We believe this is caused by the lack of assumptions as seen in other filters, keeping some amount of noise in order to make sure no proper data is lost. We can see in Figure 48, as our filter stays as the last value despite filtering, meaning no unnecessary moves are made and our new output defaulted to the original output.

Table 15

*Filter Comparison*

Filter	PHM Test Score	Original Score	Reduction %
Polynomial	2,700.20	3,285.91	17.82%
Butterworth	2,739.74	3,285.91	16.62%
Savitzky-Golay	2,260.69	3,285.91	31.20%
Kalman Filter Ensembles [1]			
Kalman Filter (KF) Ensemble	5,590.03	6,103.46	8.41%
Switch KF Ensemble	2,922.33	6,103.46	52.12%

When comparing our filter's performance with the performance of Lim's Switching Kalman Filter (SKF) Ensemble, we find that the SKF Ensemble out-performs our filters by at least 20%. However, the jump performed by their filter began at 6,101.46, almost double the size of our best model before aggregating. This could lead to worst performance with ours or low-scoring model, as seen with other methods. However, more experimentation



must be done to confirm this new hypothesis.

## Chapter 5

### Conclusion

In the beginning of this thesis, we discussed the importance of RUL estimations and how they are a modern problem in prognostics and engineering. We also discussed the common methods used, such as similarity-based approaches [5, 6, 10], feedforward neural networks and recurrent neural networks [3], as well as methods of improving feedforward neural networks using filters [1]. We then focused on what our data is, what each data feature and column represents, as well as our own models used for the experimentation.

We discussed the different methods used, their commonality, as well as how we would use each method. Our experimentation showed the improvements of scaling our target function, our failures in classification models, as well as focusing on the effectiveness of regime partitioning versus the simpler, expanded normalization method. We would also review aggregation, using our own filters and models as we compared their performances with each other and other published methods used.

From these observations and writings, we believe we've successfully improved our model with rigorous experimentation and focus, having a final score of 2260.69. We found our model to out-perform other common models based on our research using different methods that have been reproduced. This research can continue and expand to different models and methods that can further improve our results, such as the use of transferable datasets as more data. We hope that in the future this will act as a basic guideline and aid in future performance of RUL estimation models. However, there are some ways that we can better improve our model in the future as well as looking into more general models for

working with several datasets.

## 5.1 Future Work

From our experiments, we have explored different options for improving our data and model for RUL estimations. This had us focus on a breadth-first search as we attempted different methods both new and old in order to have a better understanding of the problem in general. Although this led to our previously discussed experiments, we still have other ideas, hypotheses, and implementations that we would wish to see fleshed out in the future.

**5.1.1 Transferability of datasets.** We previously showed that regime partitioning doesn't improve our score more than expanded normalization for the PHM dataset, but it does allow a stronger transferability between datasets of different operating conditions and fault modes. We wish to expand this topic on the transferability between datasets within later research, using multiple datasets for training and ways to improve and detect properties of models.

We have done this within our own research briefly, where training with C-MAPSS 2 and PHM has improved our score for our PHM training sets, for expanded normalized data. However, we wish to continue this experimentation in hopes of combining more data from different datasets will consistently improve our results. This would allow for more data to be preprocessed and added to further improve our model, but also allow the creation of an effective, generalized model for any dataset.

**5.1.2 Searching for a better scaling multiplier.** In our experiments, we consistently used a scaled target function to improve our training. This scaled multiplier that we used was the maximum RUL for the dataset, giving us a maximum of 1 and a minimum

of 0. Although this method was more effective than the kinked target function and basic target function, we found an interesting pattern if we took this further.

Let us start with a multiplier of 1, making our target function the original, basic one defined in chapter 2. We can train a model using this target function, score, and repeat with an incremented multiplier. By doing this over and over, we find a pattern emerges where a smaller score is found for a given multiplier. This score would also slowly increase in correspondence with an increasing multiplier.

We can also see improvements from C-MAPSS 3 when using C-MAPSS 1, where we can score C-MAPSS 3 lower than C-MAPSS 1 using the C-MAPSS 1 training set. This is incredibly impressive especially when considering that C-MAPSS 3 is a more difficult dataset than C-MAPSS 1. We may also see similar improvements between C-MAPSS 2 and C-MAPSS 4 as well.

However, we chose not to chose any of these results as we did this late within our experimentation phase and used our testing dataset to show this instead of a separate validation set. We would rather use this separate validation set and include the PHM datasets as it would further validate our methodology and prevent any form of snooping with our testing datasets.

**5.1.3 Incrementing our target function.** As defined in the original PHM '08 competition, our model should estimate the number of cycles *after* our current cycle. This would mean our last cycle would have an RUL of 0, our second to last cycle being 1, and so on [8]. However, when experimenting with our target function we found an improvement with our results when increasing our basic RUL target function by 1 before scaling.

When using a 25x13x1 FNN model, we found that the original, scaled target function gave us a score of 3788.18, but when using our incremented, scaled target function we found an improved score of 3439.87, an improvement by over 300 points. We also found this to improve not only our PHM dataset, but all of our datasets. We are unsure whether this means we are mostly under-estimating and doing this would work against going underneath our curve, or whether it simply improves our model output's structure somehow. We are hoping to explore this effect more in the future and see whether we can search for a better target function using these methods.

**5.1.4 Preprocessed aggregation.** In our experiments we used the inclusion of the cycle number as a way to perceive time within our model. More than this parameter being an extra column in each data point, it can also act as its own linear function for each unit. When imagining the cycle number as a model instead of a piece of data we find more possibilities emerge.

One that has been discussed before is the use of an exponential curve regression for our input data, having major sensors be fitted to a curve for better clarity [6]. This might be comparable to our experiments with post-processed aggregation and filter, where we used a 3rd order polynomial to fit our original output. We may attempt to generate our exponential curve similarly to our post-processing polynomial as well as do similar experiments with filtering algorithms in order to see how well our model performs with filtered inputs.

However, due to time constraints we were unable to perform any preprocessing aggregation and filtering with our datasets, leaving this as something we hope to experiment with in the future.

## References

- [1] P. Lim, C. K. Goh, K. C. Tan, and P. Dutta, “Estimation of remaining useful life based on switching kalman filter neural network ensemble,” in *Ann. Conf. Prognostics Health Manag. Soc*, pp. 1–8, 2014.
- [2] E. Ramasso and A. Saxena, “Performance benchmarking and analysis of prognostic methods for cmaps datasets.,” *International Journal of Prognostics and Health Management*, vol. 5, no. 2, pp. 1–15, 2014.
- [3] F. O. Heimes, “Recurrent neural networks for remaining useful life estimation,” in *Prognostics and Health Management, 2008. PHM 2008. International Conference on*, pp. 1–6, IEEE, 2008.
- [4] E. Ramasso, “Investigating computational geometry for failure prognostics.,” *International Journal of Prognostics and Health Management*, vol. 5, no. 1, p. 005, 2014.
- [5] T. Wang, J. Yu, D. Siegel, and J. Lee, “A similarity-based prognostics approach for remaining useful life estimation of engineered systems,” in *Prognostics and Health Management, 2008. PHM 2008. International Conference on*, pp. 1–6, IEEE, 2008.
- [6] T. Wang, *Trajectory similarity based prediction for remaining useful life estimation*. PhD thesis, University of Cincinnati, 2010.
- [7] L. Peel, “Data driven prognostics using a kalman filter ensemble of neural network models,” in *Prognostics and Health Management, 2008. PHM 2008. International Conference on*, pp. 1–6, IEEE, 2008.
- [8] A. Saxena and K. Goebel, “Phm08 challenge data set,” *NASA Ames Prognostics Data Repository (<http://ti.arc.nasa.gov/project/prognostic-data-repository>)*, NASA Ames Research Center, Moffett Field, CA (consulted 2014-02-15), 2008.
- [9] A. Saxena, K. Goebel, D. Simon, and N. Eklund, “Damage propagation modeling for aircraft engine run-to-failure simulation,” in *Prognostics and Health Management, 2008. PHM 2008. International Conference on*, pp. 1–9, IEEE, 2008.
- [10] J. Lam, S. Sankararaman, and B. Stewart, “Enhanced trajectory based similarity prediction with uncertainty quantification,” *PHM 2014*, 2014.
- [11] V. Nair and G. E. Hinton, “Rectified linear units improve restricted boltzmann machines,” in *Proceedings of the 27th international conference on machine learning (ICML-10)*, pp. 807–814, 2010.
- [12] G. E. Hinton, N. Srivastava, A. Krizhevsky, I. Sutskever, and R. Salakhutdinov, “Improving neural networks by preventing co-adaptation of feature detectors,” *CoRR*, vol. abs/1207.0580, 2012.

- [13] B. J. Frey and D. Dueck, “Clustering by passing messages between data points,” *Science*, vol. 315, no. 5814, pp. 972–976, 2007.
- [14] G. Welch and G. Bishop, “An introduction to the kalman filter,” 1995 (Accessed in March 2017). [https://www.cs.unc.edu/~welch/media/pdf/kalman\\_intro.pdf](https://www.cs.unc.edu/~welch/media/pdf/kalman_intro.pdf).
- [15] S. Butterworth, “On the theory of filter amplifiers,” *Wireless Engineer*, vol. 7, no. 6, pp. 536–541, 1930.
- [16] W. H. Press and S. A. Teukolsky, “Savitzky-golay smoothing filters,” *Computers in Physics*, vol. 4, no. 6, pp. 669–672, 1990.